

Portable Multiplex Optical Assays

Ahmet F. Coskun,* Seda Nur Topkaya, Ali K. Yetisen, and Arif E. Cetin*

Global health issues are increasingly becoming critical with high fatality rate due to chronic and infectious diseases. Emerging technologies aim to address these problems by understanding the causes of lethal conditions and diagnosing symptoms at early stage. Existing commercial diagnostics primarily focus on single-plex assays due to ease-of-use, simplicity in analysis, and amenability to mass manufacturing. Many research grade devices have utilized only a few molecular and morphological signatures in bodily fluids. However, multiplex devices can improve accuracy, sensitivity, and scalability of research and diagnostic devices. This review presents multiplex assays that utilize optical, electrical, and chemical methods and materials that have the potential to improve portable point-of-care diagnostics. The critical role of emerging optical and complementary assays with multiple contrast mechanisms is investigated to enable highly multiplex analysis in field settings. Multiparameter portable devices for field applications toward health monitoring, food testing, air quality monitoring, and microanalysis in other extreme conditions are examined. Current trends indicate the need for validation of health diagnosis based on a large number of biomarkers in randomized clinical trials. Advanced digital analysis, crowd-sourced solutions, and robust user interfaces will become an integral part of the connected global health systems and personalized monitoring platforms.

1. Introduction

Centralized facilities such as hospitals have provided healthcare services at increasing cost. The capacity and affordability of these central hubs fail to meet the growing need. To enhance global penetration of health services, point-of-care devices and solutions have been demonstrated.^[1] Handheld devices,^[2] smartphone readers,^[3] and wearable monitoring interfaces^[4] have become readily available to provide health-related information in remote locations. Among many others, blood tests can now be

performed at home and results can be integrated by online interfaces.^[5] The test results and diagnostic information can be analyzed by the medical professionals from remote locations, improving the connectivity of central hubs to the public venues.

Numerous scientific discoveries have been made in advanced settings and well-equipped laboratories. The necessity and complexity of these environments limit access to research equipment worldwide. Thus, decentralization of research laboratories has become an alternative solution to improve access to experimentation in field conditions. For instance, a paper origami microscope^[6] that fit into a palm of a student made a powerful investigation tool for environment and materials. A detailed analysis of sound recordings by smartphones enabled identification of distinct mosquitoes.^[7] These field-deployable devices and platforms have stimulated emergence of citizen scientists, a population that collectively performs scientific inquiries in public settings.

Rich biomolecular measurements from field-portable devices improve the quality of results in terms of accuracy and depth. Monitoring multiple blood markers has enabled diagnostic precision and thorough scientific investigation of blood constituent in patients. Therefore, field-deployable devices should ideally have multiplexed detection of target specimens. Design of such multiplexed detection technologies requires decent complexity at low cost for wide-scale adoptability.


In this article, we provide an overview of field-compatible devices with high parameter analysis capabilities for both health monitoring purposes and scientifically enlightening

Dr. A. F. Coskun
Department of Radiology
Molecular Imaging Program at Stanford
Stanford University School of Medicine
Stanford, CA 94305, USA
E-mail: coskun@stanford.edu

Prof. S. N. Topkaya
Department of Analytical Chemistry
Faculty of Pharmacy
Izmir Katip Celebi University
Izmir 35620, Turkey

Dr. A. K. Yetisen
Department of Chemical Engineering
Imperial College London
London SW7 2AZ, UK

Dr. A. E. Cetin
Izmir Biomedicine and Genome Center
Izmir, Balçova 35340, Turkey
E-mail: arifengin.cetin@ibg.edu.tr

 The ORCID identification number(s) for the author(s) of this article can be found under <https://doi.org/10.1002/adom.201801109>.

DOI: 10.1002/adom.201801109

applications. Optical, electrical, and chemical design strategies are also highlighted. Along with the critical perspectives on device performance and economics, translation potential of each device is provided.

2. Optical Devices and Materials

Optical interfaces allow rapid and minimally invasive interrogation of biological specimens.^[8] Interactions of light with matter enable sensing mechanisms to detect minute variations of target samples at high sensitivity. The use of simple components such as light-emitting diodes (LEDs) and cost-effective detectors in optical designs provides compact and affordable devices. In this section, we present emerging platforms that provide multiplex detection in optical devices for field applications.

2.1. Optical Devices with Chemical Interfaces

Optical readers, when combined with the chemical methods, enable analytical characterization devices for biosensing needs in environmental screening, food safety, and health diagnostics. Among others, fiber optics have received considerable attention due to its high sensitivity to the local environment at the vicinity of light travelling interfaces.^[9] While the sensing principles differ in their operation mechanisms, the general strategy is to rapidly detect the presence of a target such as metabolites, nucleic acids, proteins, ions, or microorganisms based on a contrast generation around fiber surfaces.^[10] Evanescent wave fiber biosensors are preferred for sensing as they rely on confined light around the outer region of a fiber that is generated upon reflection of light within the fiber inner interfaces.^[11,12] Since fibers are compact and lightweight, fiber biosensors present ideal platforms for field use. Many of these physical devices are also interfaced by a computer integration, portable and compact units, as well as smartphone-based readouts. Despite the fact that many of these studies have targeted single molecule or cell type, simultaneous screening of multiple targets makes them valuable for more comprehensive screening in health and environmental applications. A simple solution for multiplexed detection was demonstrated by partitioning the sample into multiple fibers that were specifically modified to detect foodborne pathogens (Figure 1A).^[13] Chemical functionalization of fiber interfaces by streptavidin allowed conjugation of biotinylated antibodies to capture particular pathogen of interest. This multiplex fiber biosensor detected *Listeria monocytogenes*, *Escherichia coli* O157:H7, and *Salmonella enterica* in meat samples with 100 cfu 25 g⁻¹ sensitivity based on fluorescent readout. In this multipathogen fiber sensor design, adding separate fiber sensors with an antibody library for a large set of antigens will boost multiplexing.

Fiber sensors have successfully allowed compact biosensing devices in various applications. However, their physical interfaces are sensitive to any mechanical vibrations and movement artifacts that typically occur in field settings. To provide an alternative platform to this important need, lateral flow assays have been developed to detect chemical and biological targets using a control region and an active sensing region.^[14] These lateral



Ahmet F. Coskun is an Instructor of Radiology at Stanford University School of Medicine. He researches spatial genomics and proteomics, computational immunology, systems biology, precision medicine, and biophotonics. His research centers on single cell analysis, subcellular imaging, and multiplex assays using

interdisciplinary quantitative tools. He trained at California Institute of Technology for his postdoctoral work. He holds a Ph.D. degree from the University of California, Los Angeles, CA, and a bachelor degree from Koc University, Turkey.



Arif E. Cetin is a Research Group Leader in Izmir Biomedicine and Genome Center in Izmir, Turkey. He received his Ph.D. degree from Boston University, Boston, MA. He worked as a postdoctoral associate at EPFL, Switzerland and MIT, Massachusetts, MA and research scientist at Omniome, San Diego, CA.

Dr. Cetin pursues research on optical nano-biosensors integrated with microfluidics, handheld biosensors for high-throughput and multiplexed biosensing, electromechanical sensors for growth rate cytometry, and label-free techniques for DNA sequencing.

flow assays are used for convenient testing at sufficient sensitivity in public venues. Compared to other complex assays such as ELISA immunoassay or polymerase chain reaction (PCR), lateral flow methods do not require any complex equipment or advanced training, enabling practical applications in field medicine. Typical lateral flow assay devices are designed in the form of a test strip (mostly in the paper format) to detect only one target together with a control region. Target samples are chemically conjugated on an initial pad as they flow through the device, followed by capturing conjugated samples on an accurate binding region to specific primary antibodies (test line) and nonspecific binding to a nontarget antibody (control line). Direct approach to visualize multiple targets is to use different test strips (with distinct antibody libraries) from the same sample and combine results from multiple readouts. An integrated approach was created by a cellphone-based rapid diagnostic test reader as a universal imaging and analysis platform (Figure 1B).^[15] Multiple lateral flow assay tests for HIV, tuberculosis, and malaria were digitally quantified by this

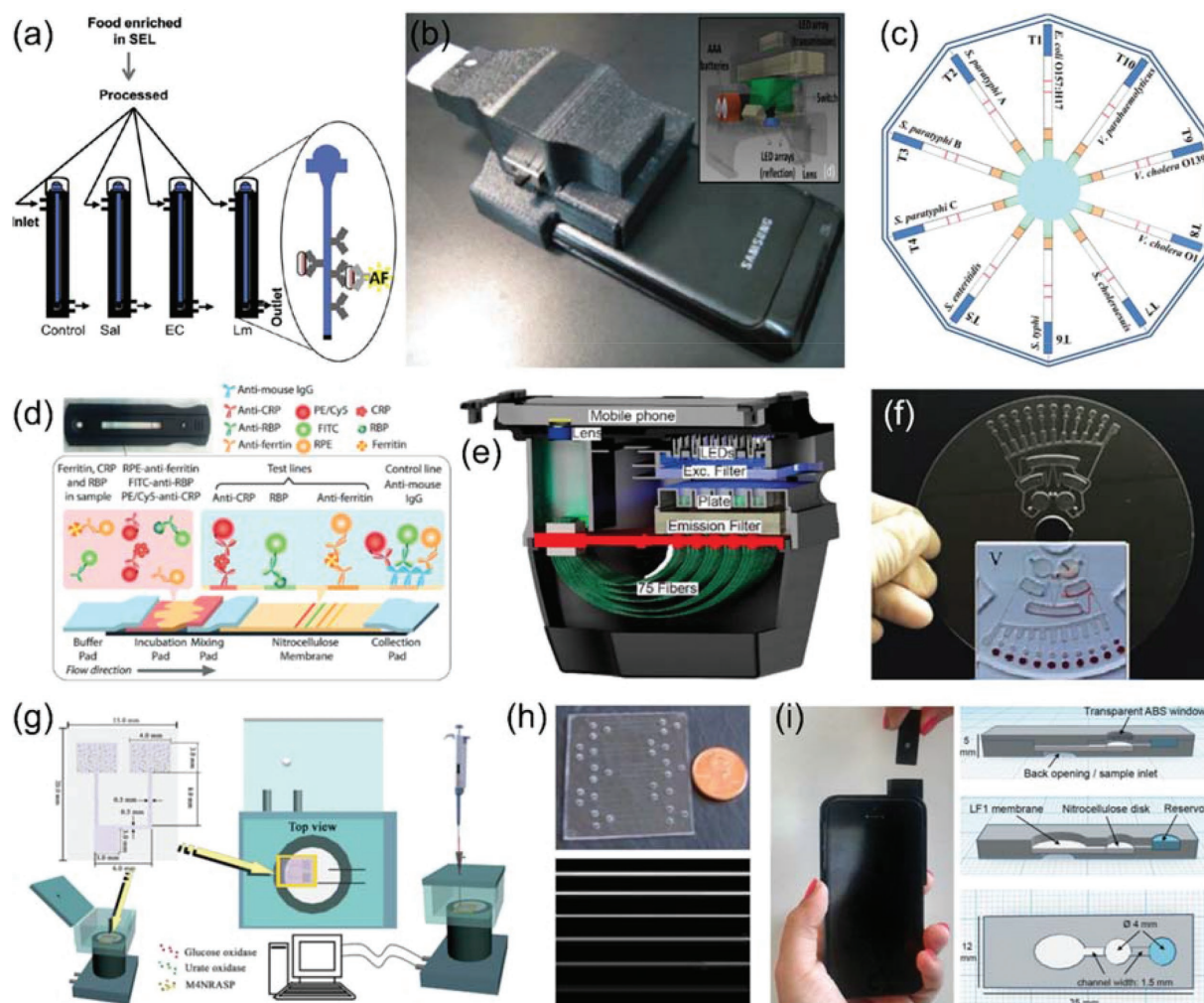


Figure 1. Optical chemical devices. a) Schematic of the multiplex fiber biosensor. b) Cell phone-based rapid-diagnostic-test (RDT) reader platform that can work with various lateral flow immuno-chromatographic assays. Inset: Schematics of RDT platform. c) Design of lateral flow assay to detect ten food pathogens. d) Fluorescent lateral flow assay for detection of three biomarkers. e) Smartphone-based plate reader for isothermal and multiplex nucleic acid detection. f) An amplification assay for multiplex analysis of six bacteria in microfluidic disk format. g) Schematic diagram and assay procedure of the microfluidic paper-based chemiluminescence analytical device with a simultaneous, rapid, sensitive, and quantitative response. h) Top: Photo of plastic microfluidic immunosensor for rapid, reliable, and on-the-spot detection of disease biomarkers in human sera. Bottom: Chemiluminescence image for different concentrations of C reactive protein (CRP). i) A waveguide-based multiparameter analysis. Reprinted from refs. [13] (a), [15] (b), [16] (c), [17] (d), [19] (e), [21] (f), [23] (g), [25] (h), and [27] (i) with permission: Copyright 2012, Elsevier Ltd. (a); Copyright 2012 and 2011, The Royal Society of Chemistry (b and g); CC-BY 4.0 open access publication (c and f); CC-BY-NC-ND 4.0 open access publication (d); ACS AuthorChoice License open access publication (e); Copyright 2006, Springer Science Business Media (h); Copyright 2014, American Chemical Society (i).

smartphone reader, providing creative platforms for research and diagnostics.

Recently, a multiplexed strategy was introduced to simultaneously measure ten distinct foodborne pathogens.^[16] This sensor design included a common sample loading region and then distribution to ten different arms in the shape of a disk (Figure 1C), providing a practical single step testing without sophisticated sample preparation. The reagents have also been unified to avoid variations due to the labeling or target type differences. For more than 200 food samples, reproducible experiments were achieved in the range of 10^4 – 10^5 CFU mL⁻¹ detection sensitivity. Another multiplexed lateral flow assay was developed based on fluorescent reporters (Figure 1D). Three target proteins in the blood serum, ferritin, retinol-binding

protein (RBP), and C reactive protein (CRP), were detected by a multicolor test strip to monitor iron and vitamin A deficiency.^[17] Similar to the cellphone-based integrated reader,^[15] this multiplexed sensing platform was analyzed by a smartphone interface.

A higher sensitivity with field-portable design was demonstrated using isothermal (mostly room temperature) amplification strategies. A loop-mediated and toehold-assisted nucleic acid amplification methods have boosted the fluorescent readout.^[18,19] While the operation principle of this chemical assay was relatively complex, target samples were conjugated to a nucleic acid capture probe, which was then amplified by a series of reactions without the need for thermal cycling to overcome a drawback of portable designs. Owing to the

intense signal, a portable smartphone-based plate reader^[20] was then used to image and quantify target nucleic acids such as viral RNA for *Influenza* (Figure 1E). The similar isothermal assay was employed in a microfluidic disk format to detect six different bacteria (Figure 1F).^[21] In this platform, distinct bacterial strains were detected in real time within a total assay time of 70 min, an advance for field applications as compared to standard 24 h bacterial culture protocols.

Another advantageous optical design is chemiluminescence detection for multiplex optical approaches.^[22] The reagents generate self-luminescence signal that correspond to analyte concentrations, which can then be detected by a digital camera without the need for any other optical illumination components. Recent demonstration of chemiluminescence assays included paper microfluidics. Oxidase enzymatic reactions were used to measure glucose and uric acids in artificial urine samples with 0.14 and 0.52 mmol L⁻¹ detection limit, respectively (Figure 1G).^[23] Because this approach necessitates only a luminescence reader, the reduction in the optical design principles (no lasers or LEDs) provided ideal platforms for portability.

Further simplification in the optical design was also demonstrated by integrating lensless imaging^[24] with chemiluminescence assays. A combination of enzymatic assays for detection of alkaline phosphatase levels, a nucleic acid labeling approaches for Parvovirus B19 DNA, and horseradish peroxidase measurements that were all detected in the digital camera without lens-based coupling. Instead of using fluorophore chemistry, these assays generated self-luminescent signal without excitation of samples. Only a simple fiber array was used to collect and concentrate the luminescent signal to the camera pixels. Attomole detection limit for proteins and femtomole sensitivity for nucleic acids were achieved in this integrated multiplex device. An integrated approach was also designed for microfluidic format chemiluminescence assays that were captured on photographic films and imaged directly by a camera (Figure 1H).^[25] C reactive protein (CRP) in serum samples were measured at 0.858 mg L⁻¹ sensitivity levels with this rapid chemiluminescence optical method. In combination with firefly inspired and long-term sustainable hydrogels,^[26] chemiluminescent assays were poised to impact highly sensitive and multiparameter optical designs for field applications.

To enhance digital connectivity and analysis, chemiluminescence and bioluminescence were coupled to smartphone readers. Total bile acids were measured by bacterial luciferase system and total cholesterol was detected by horseradish peroxidase methods within a 3D-printed attachment on the camera unit of a smartphone (Figure 1I).^[27] For portable designs, luciferase presented an ideal solution for light generation based on a substrate (luciferin) without additional light delivery to the sample. Using a rapid sample preparation in 3 min, sensitive detection of analytes in blood serum at 20 mg dL⁻¹ sensitivity and in oral fluids with 0.5 μmol L⁻¹ detection limit. A similar strategy was implemented in the form of lateral flow assays to measure cortisol in saliva by smartphone imaging.^[28] A forensic tool was also developed by smartphone imaging of Artemisinin-Luminol ions in bloodstains through chemiluminescence of sodium perborate and hydrogen peroxide.^[29]

2.2. Optical Devices with Engineered Nanomaterials

Conventional optical platforms are limited to resolve structures smaller than the wavelength of light due to the diffraction limit since the subwavelength information carried by the evanescent fields are lost before forming an image while passing through media with different permittivity values.^[30] Recently, plasmonics has emerged as a solution to compensate this loss due to evanescent field to restore images below the diffraction field. The unique optical properties of surface plasmons originate from the collective free electron oscillations of noble metals and these surface wave oscillations confine light at nanoscale.^[31] The electromagnetic field of light confined at the metal surfaces, in the form of surface plasmons, enhances the light-matter interaction at nanoscale. Therefore, the increase in the refractive index of the medium around the metal, due to the addition of biomass on the surface, shifts the surface plasmon excitation wavelength. This spectral shift is then used to determine the presence of targeted biomolecules.^[32] Plasmonic sensors enable label-free biodetection without the need for fluorescence tags.^[33] The gold standard plasmonic sensing method, surface plasmon resonance (SPR), utilizes a coupling mechanism to excite surface plasmon on a thin metal film placed on top of a prism. This mechanism provides a highly sensitive biodetection with femtomolar (fM) concentration limits and high protein kinetics with k_a between 10³ and 10⁷ M⁻¹ s⁻¹ and k_d between 10⁻⁵ and 1 s⁻¹.^[34] Recently, lightweight and low-cost portable SPR platforms were developed, providing rapid detection for field settings. These platforms utilize a miniaturized prism coupling mechanism with a sensor chip integrated to a microfluidic chamber. The reflected light (laser or LED sources) from the chip was collected with a photodetector, and the spectral variations due to analyte binding on the flat metal sensor chip were processed with a laptop or a cell phone, providing the sensing data to the user.^[34-36] For instance, a portable fiber-optic SPR platform was integrated to a smartphone (Figure 2A).^[34] Optical components were connected by an optical fiber, where the light emitted from an LED source propagated within the fiber and the reflected light from the gold SPR chip was detected by a cell phone camera (Figure 2B). The spectral shift within the reflection response (or the surface plasmon excitation wavelength) causes variations within the reflected light intensity since the reflection at the LED dominant wavelength is different in the presence of biomolecules. The portable SPR platform exhibited a detection limit of 47.4 × 10⁻⁹ M, which is a very suitable sensitivity level for field applications.

Although these efforts on portable SPR platforms introduced highly sensitive label-free biodetection for field settings, due to their optically sensitive and bulky prism coupling mechanism, these systems suffer from throughput.^[37] To address this need, nanoscale structures in the form of metallic particles and apertures have received significant attention due to their unique ability to excite strongly confined local electromagnetic fields with high nearfield enhancements.^[38] In particular, nano-hole arrays fabricated through thin metal films overcome the momentum mismatch between surface plasmons and free space photons, and enable extraordinary light transmission through the grating order of the array.^[39] These aperture arrays support local fields with extreme intensity enhancements that

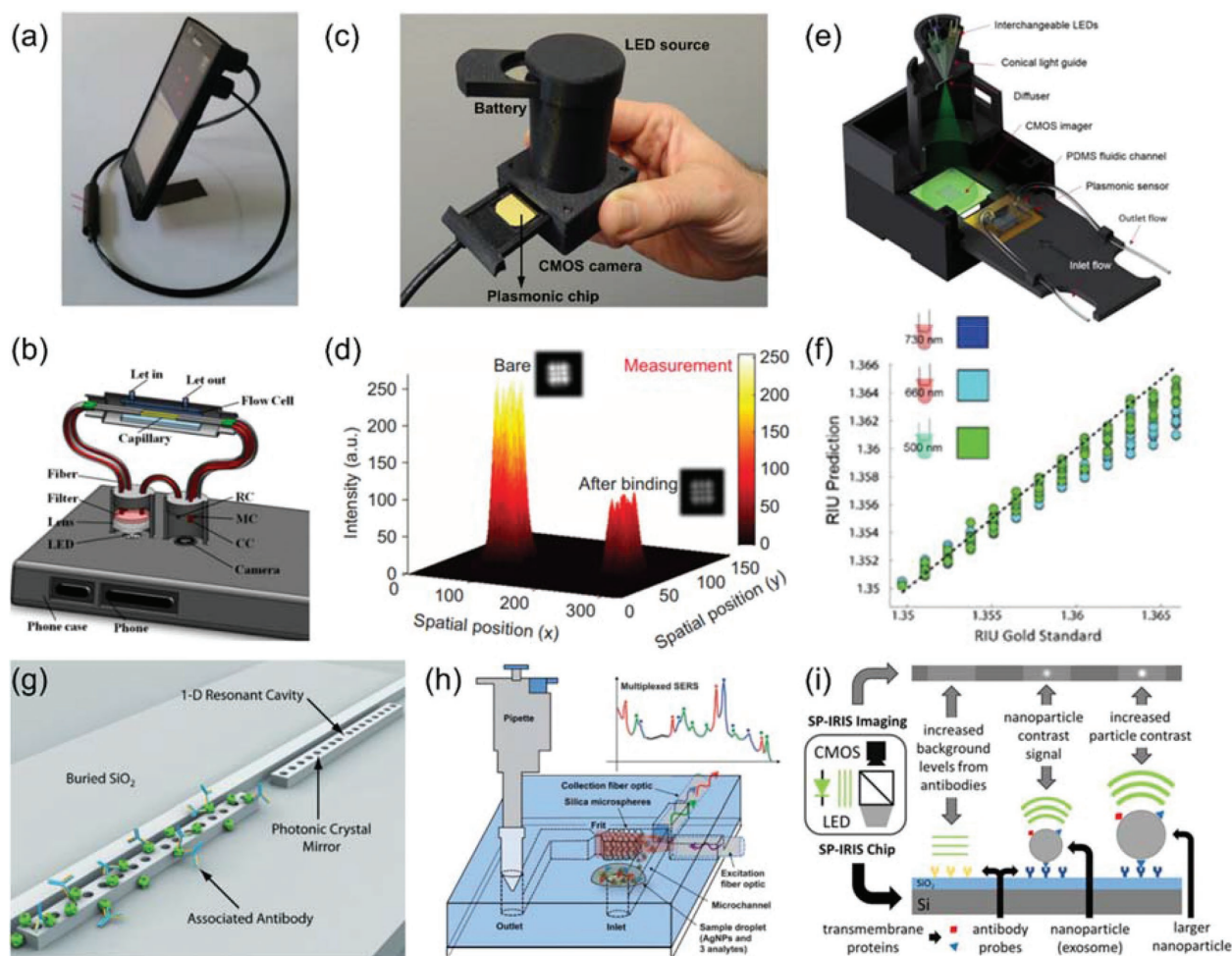


Figure 2. Optical devices with engineered nanomaterials. a) Photograph and b) schematic illustration of the SPR sensor integrated to a smartphone. c) Picture of the plasmonic lens-free handheld biosensor. d) Portable sensor detects the targeted biomolecules by monitoring the change in the diffraction pattern intensity. e) Schematics of the plasmonic reader employing a machine learning algorithm. f) Linear LED model for minimum refractive index sensing error. g) Optofluidic device with nanocavity. h) An optofluidic SERS device for multiplex detection in water. i) High throughput interferometric reflectance biosensor. Reprinted from refs. [36] (a,b), [43] (c,d), [45] (e,f), [49] (g), [54] (h), and [59] (i) with permission: CC-BY 4.0 open access publication (a,b,i); CC-BY-NC-ND open access publication (c and d); Copyright 2017, American Chemical Society (e and f); Copyright 2009 and 2012, Royal Society of Chemistry (g and h).

are associated with the cavity modes of the nanoapertures. They are also highly sensitive to minute changes within the refractive index of the medium in the vicinity of the metal surface as they confine light to the sensing surface, extending extensively into the surrounding medium.^[40] More importantly, the grating coupling mechanism allows surface plasmon excitations even at normal incidence so that this collinear configuration enables biodetection through much simpler optical setups that are not sensitive to the alignment of the source and the chip.^[41] The accumulated biomass on the sensing surface is detected by the spectral shift within the transmission response of the nanohole arrays, for example, read out by a spectrometer. This configuration is also compatible with imaging devices within an array format, making them an ideal candidate for high-throughput and multiplexed sensing applications.^[42] Utilizing imagers instead of spectrometers dramatically increased the throughput as the sensors on the plasmonic chips could be evaluated simultaneously rather than sequentially.^[37] Recently,

efforts to use this phenomenon to develop portable plasmonic sensors were achieved by employing affordable camera and light source settings, replacing sophisticated microscopy setups composed of optical filters, light source, and expensive cameras. For example, a cost-effective handheld biosensing platform was integrated to plasmonic nanohole array chips containing sensors in microarray format and a lens-free computational microscopy platform.^[43] The platform utilized a complementary metal-oxide-semiconductor (CMOS) imager to record plasmonic lens-free diffraction patterns that were illuminated by an LED source, spectrally tuned to the transmission resonance of the nanohole arrays (Figure 2C). The system determined the spectral shifts within the transmission resonance, due to the presence of the biomolecules on the gold sensing surface, through monitoring the diffraction pattern intensity change (due to the mismatch between LED and nanohole response) taken by the CMOS camera (Figure 2D). The system enabled detection of protein layers down to 3 nm. By integrating the

lens-free platform to large-scale microarray plasmonic chips, high-throughput and multiplexed detection of different protein layers and quantitative concentration analysis of same protein molecules were also performed all in the same platform. Integrating the handheld device to a low-cost microfluidic biochip, protein binding kinetic analyses with SPR quality have been demonstrated.^[44] Instead of analyzing spectral shifts, this portable design relied on reduction of transmission signals that were detected by a CMOS camera during the measurement of binding kinetics. Recently, a machine learning framework was introduced to select the optimum source and plasmonic chip combination through a minimum-error refractive index prediction model.^[45] Modular design of the portable multispectral plasmonic reader was presented (Figure 2E). Linear models were used for refractive index prediction by using LED light sources with different emission wavelengths, illuminating a plasmonic chip (Figure 2F). This tool could be an ideal universal standard for the plasmonic community to design portable sensors providing reliable sensing data for resource poor settings.

Another approach is to utilize optofluidics (optics and microfluidics) for multiplex detection.^[46] Optical design enables sensitive measurements by the use of light engineering and, at the same time, microfluidic interfaces allow rapid sample exchange. One implementation of such a design was a Young's interferometric detection integrated to microfluidics.^[47,48] In this platform, the waveguide surface was coated with antibodies and the specific binding of analytes on the surface varied the evanescent fields of the guided modes. This variation triggered a phase change in the interference pattern. Analysis of the interference pattern was then used to determine the amount of adsorbed analytes on multiple channels, providing multiplexing. Human serum albumin (HSA) and viruses were measured. High sensitivity of interferometric detection enabled 20 fg mm⁻² of HSA markers and 850 particles mL⁻¹ of herpes simplex virus type 1. Another optical design was the use of photonic crystals^[49-51] to confine light for detection of antigens (Figure 2G). The system employed evanescently coupled 1D photonic crystal resonators, where the accessible optical field inside the holes of photonic crystal was very strong. Therefore, the light-matter interactions were enhanced to yield high sensitivity. By localizing the optical field to mode volumes on the order of a wavelength cubed, a detection limit on the order of 10s of attograms total bound mass was shown. In this device, Interleukins 4, 6, and 8 were simultaneously measured by an optofluidic device with a sensitivity level of 63 ag total bound mass. Additional designs with optofluidic fiber resonators were also demonstrated for multiplexed sensing applications.^[52] The system utilized a self-referencing optofluidic ring resonator, where the mode-splitting separation generated on a coupled ring resonator was monitored such that the common-mode noise was suppressed by two orders of magnitude. The resonator-based biosensor system detected bovine serum albumin with a detection limit on the order of 15 × 10⁻¹⁵ M. Introducing more detection paths in the optic designs would increase multiplexing in optofluidic assays.

A complementary optical method was surface enhanced Raman spectroscopy (SERS) to detect targeted analytes within compact units. SERS provides an enhancement in the optical

platform to improve the limit of detection (LOD).^[53,54] One demonstration is the monitoring of aquaculture fungicides, as low as detection of 5 part-per-million (ppm) methyl parathion, 0.1 part-per-billion (ppb) malachite green, and 5 ppb thiram in water (Figure 2H). Another advance in this platform is to alleviate the use of bulky fluidic pumps with a physical pipette with negative pressure used for sample loading. Using inkjet printing, a paper-based implementation of SERS approach was also demonstrated to detect as low as 95 fg of Rhodamine 6G (R6G), 413 pg of the organophosphate malathion, 9 ng of heroin, and 15 ng of cocaine.^[55,56]

Most of these optical devices have relied on spectroscopic analysis. However, a direct imaging of transmission/reflection signal was also utilized for sensing a wide range of biomarkers and other nanoscale targets. An interferometric imaging^[57,58] was shown to monitor analytes based on signal enhancement of nanoparticles located on a silicon substrate with silicon dioxide coating (Figure 2I). In this design, incoming light was reflected off of the silicon substrate through the thin silicon dioxide layer to create an optical signature in the form of an interference pattern. Using antibodies on the silicon dioxide layer, target molecules were captured within the device, providing a shifted reflectance spectrum. Based on an optical path length calculation, the number of bound molecules was calculated to determine the concentration of analytes. As an example, exosomes were classified by such an interferometric imaging design using CD81, CD63, and CD9 antibodies.^[59] A sensitivity level of 3.94 × 10⁹ particles mL⁻¹ was demonstrated for exosomes that were isolated from HEK 293 cell lines. The ultimate detection limit of interferometric biosensors is single proteins,^[60] although the optical setup requires significant miniaturization for field applications.

2.3. Optical Genomic Devices

DNA sequencing is a key tool for diagnostic technologies. Determining the base sequence in DNA is important for investigating gene functions, their association with diseases, and developing personalized treatments.^[61-63] Different sequencing technologies have been introduced, utilizing optical readout mechanisms, including fluorescently tagged nucleotides and ligation of fluorescent oligonucleotides.^[64,65] With the development of next-generation sequencing (NGS) techniques, sequencing cost dramatically decreased as these methods determined millions of sequences with a single sequencing run. Recent commercial optical NGS platforms, that is, Illumina sequencing, utilized fluorescently labeled nucleotides and serial polymerase-catalyzed extension, where the correct base was determined by a fluorescence signal.^[66] Sequencing by Oligonucleotide Ligation and Detection (SOLiD) based genomic analysis utilized arrays of amplicons on beads, which were subjected to ligation of fluorescently labeled oligonucleotide probes.^[67]

Despite the rapid progress in sequencing technology, further developments are still needed to reduce the cost as the point-of-care molecular diagnostics, a critical criterion for resource poor settings in underdeveloped countries. On the other hand, the cost of molecular analyses is still a concern in developed

countries even the benchtop medical technologies are available to patients. Therefore, there is a strong need to realize affordable diagnostic technologies that can be utilized in field settings. For instance, one effort to address these requirements was the long-read portable sequencer MinION released by Oxford Nanopore Technologies (Figure 3A), which took significant attention due its affordability and speed of data production.^[68] The technique utilized a core sensing unit and nanopore array set that comprises an electrically resistant polymer membrane. DNA bases were identified by determining the variations within the electrical conductivity as the DNA strands pass through the pore. The flow-cell unit generated 10–20 gigabytes (Gbs) of sequencing data and provided DNA sequences in real time, that is, analyses were performed during the experiment. This device was suitable for sequencing of bacteria or viruses with good accuracy, reliability, and speed, making it an ideal candidate for applications in resource-poor settings and routine tests in hospital laboratories. Recently, the leading sequencing company Illumina, Inc., released a new generation benchtop sequencer, iSeq 100, allowing affordable and accurate next-generation sequencing in any laboratory (Figure 3B). The system employed a low-cost CMOS imaging technology and accurate sequencing by synthesis (SBS) chemistry. The system provided higher data resolution as compared to Sanger and quantitative PCR sequencing and possessed stronger statistical confidence. The read length of the iSeq 100 System was 2×150 DNA base pairs with Illumina's data quality. The system was designed to conduct analyses on relatively shorter length of DNA sequence

fragments so that it eliminated requirements for low-input samples in high-throughput devices with longer and expensive procedures. It allowed proof-of-principle studies to evaluate libraries before the large-scale runs. More importantly, most of these studies on microorganisms, that is, viruses or bacteria, only need 50–100 bases read length, so iSeq 100 System is suitable to study pathological disease models in resource-poor settings in an affordable way. Portable DNA analyzer can also be used for forensic DNA testing to find similarity between suspects' DNA fragments and those of the biological evidence collected at the crime scene. Using the portable DNA analyzer could allow performing such tests in the crime scene to expedite the decision making. Recently, ParaDNA Screening System was released to use in field, at scene, or in submissions crime laboratories as a DNA screening test, that consists of a sampling device, preloaded reaction plates and detection instrument (Figure 3C). The system detected PCR amplicons to identify the presence of evidence DNA fragments. The system and its software were easy to use and produce reliable data such that a DNA analyst for decision-making was not needed. Internal databases were searched and compared as a user-friendly design. The system determined the presence of DNA from complex media including blood and saliva in 75 min.

In addition to commercial options, research efforts have reduced the cost of sequencing while improving the data quality. Recently, a cell phone-based DNA sequencer was demonstrated for point-of-care diagnostics.^[69] This device allowed DNA sequencing and in situ mutation analysis together with tissue

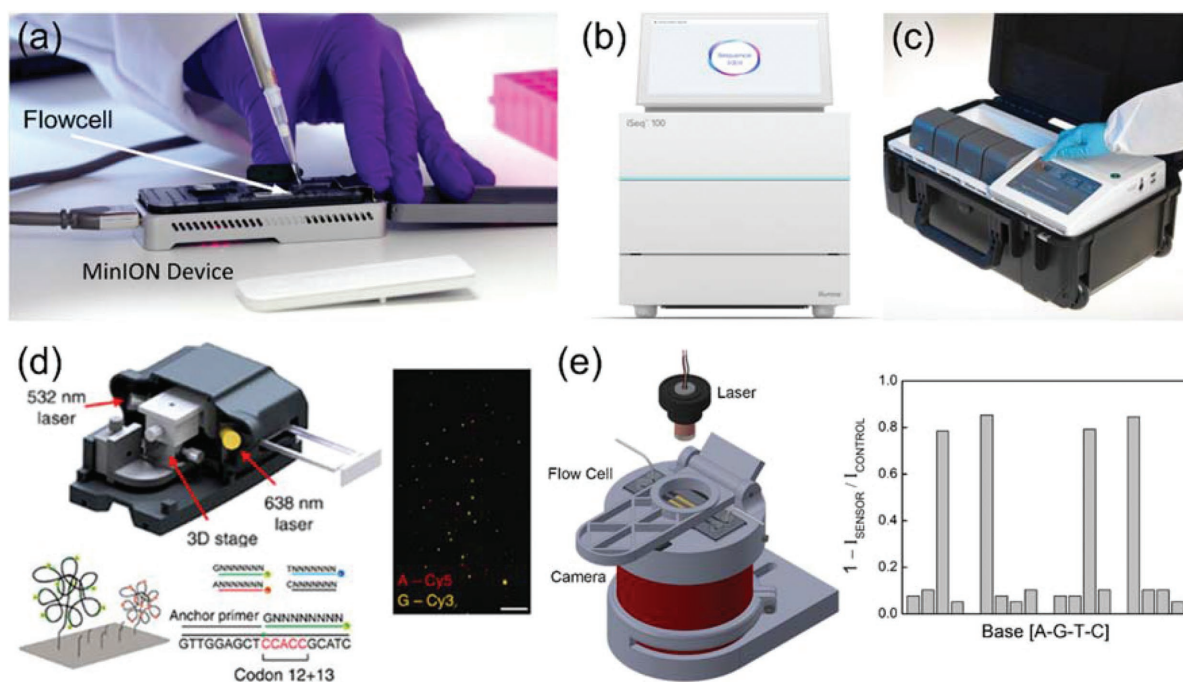


Figure 3. Optical genomic devices. a) MinION sequencer built by Oxford Nanopore (Reproduced with permission from <https://nanoporetech.com>). b) iSeq 100 sequencer built by Illumina, Inc. (Reproduced with permission from <https://www.illumina.com>). c) ParaDNA Screening System by LGC Group on-site portable forensic DNA testing (Reproduced with permission from <https://www.lgcgroup.com>). d) Top left: Schematic illustration of the cell phone-based sequencer. Bottom left: Sample preparation scheme for cell phone-based DNA sequencer. Right: Dual-color mobile phone microscope image. Scale bar, 50 μm . e) Left: Schematics of the imaging-based label-free DNA sequencing platform, employing a laser diode, a fluidic chamber, and a CMOS camera. Right: Change in the intensity of the diffraction patterns for four bases in the DNA template. Reprinted from refs. [69] (d) and [70] (e) with permission: CC-BY 4.0 open access publication (d); Copyright 2018, American Chemical Society (e).

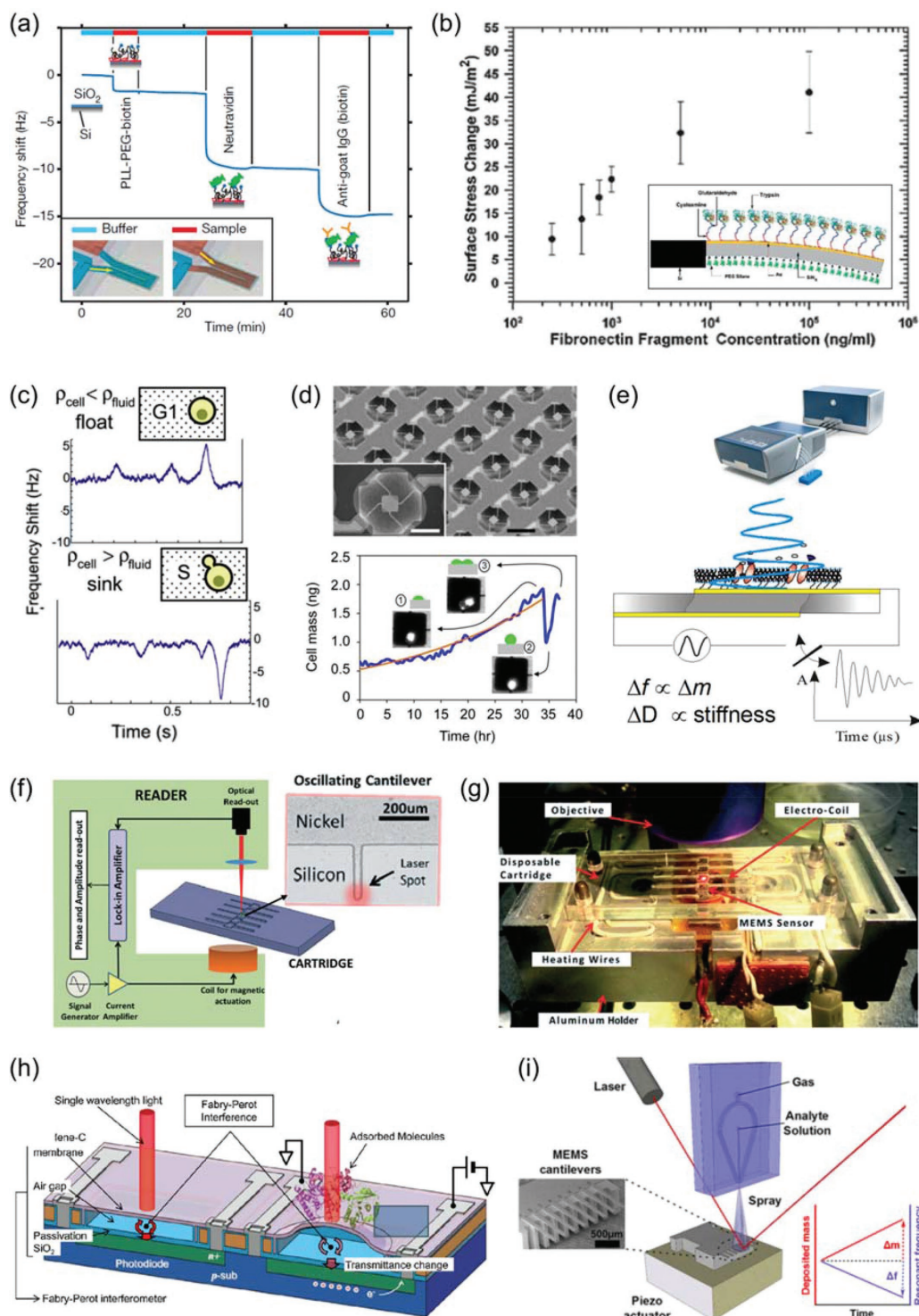


Figure 4. Optical microelectromechanical system (MEMS) devices. a) Frequency shift in the cantilever response upon attachment of biomolecules. b) Surface stress change versus fibronectin fragment concentration. Inset: Schematics of the functionalized cantilever. c) Real-time relative cell density measurement. d) SEM image of a pedestal mass measurement sensors (PMMSs). Individual cell growth measured by PMMSs. e) A commercial quartz crystal microbalance (QCM) platform, Q-Sense E4 by Q-Sense, Inc. Schematics of working principle of Q-Sense E4 (Reproduced with permission from <https://www.biointerferometric.com/qsense>). f) Schematics and g) photograph of the microelectromechanical system for multiple coagulation measurements from plasma. h) Schematics of the surface stress sensor based on a MEMS Fabry-Perot interferometer. i) Schematics of the MEMS-based dry mass sensing platform. Reprinted from refs. [71] (a), [72] (b), [78] (c), [79] (d), [81] (f, g), [82] (h), and [83] (i) with permission: Copyright 2007, Springer Nature (a); Copyright 2008 and 2017, American Chemical Society (b and i); CC BY-NC-ND 4.0 open access publication (c and d); Copyright 2015, Royal Society of Chemistry (f and g); Copyright 2013, Elsevier B.V. (h).

morphology in tumors. The system utilized a cell phone camera and two lasers for multicolor fluorescence imaging (Figure 3D). DNA fragment was selectively circularized on selector probes that were attached to the slides. The rolling circle amplification (RCA) products were sequenced by unchained sequencing by ligation chemistry. The system allowed simple and low-cost molecular information for point-of-care diagnostics in doctors' office or in resource-poor settings. The system can also be used for short DNA reading suitable for pathological disease as well as investigation of antibiotic resistance markers. The portable device has been promising to lower the cost of NGS-based diagnostics. Label-free optical technology could also serve for NGS. Consequently, a label-free DNA sequencing platform based on refractive index sensing through plasmonic nanohole arrays was demonstrated.^[70] The platform utilized sequencing by binding (SBB) chemistry for robust attachment of DNA templates on sensing surface, ensuring the correct base pairing on templates. Formation of the protein complexes, composed of template, polymerase, and the correct nucleotide, triggered a spectral shift within the plasmonic response of the gold nanohole arrays to identify the correct sequence of different DNA templates. Integrating the label-free DNA sequencing platform with an imaging device, the formation of protein complexes was monitored through changes in the intensities of plasmonic lens-free images (Figure 3E).

2.4. Optical Microelectromechanical Devices

Integrating optical readout mechanisms to microelectromechanical devices, comprehensive data could be generated for the targets by adding different parameters to the overall data, that is, mass, density, or stiffness of cell-based assays. Microelectromechanical systems are miniaturized machines with both mechanical and electronic components. One promising way of developing low-cost, compact, and reliable diagnostic and analysis platform is the use of microcantilevers. These biosensors could measure density and total mass information of an individual cell/analyte of interest. The working principle of these sensors is either by detecting the biochemical reactions on the surface of the cantilevers or the total mass change of the cantilevers upon the presence of target biomaterials. Although detection limits of these platforms are comparable with the commercial devices, they suffer from limitations that need to be addressed before these highly sensitive biosensing techniques turn into a reliable, robust, and compact commercial device with portability.

As an example, a suspended microchannel resonator (SMR) technology^[71] was demonstrated to weigh protein molecules and microorganisms, for example, bacteria. The system comprised of a low resonator mass and high-quality factor resonances to enable sub-femtogram resolution. The resonance frequency of the cantilever was dependent on its total mass. The system used the change in the resonance frequency to determine the variation in the mass due to the biomolecules binding on the resonator wall. The biomolecules binding on the resonator wall accumulated, enabling detection with high specificity defined by immobilized ligands. Frequency shift was plotted as a function of analyte binding in the order of electrostatic adsorption

of PLL-PEG-biotin, neutravidin, and attachment of biotinylated Immunoglobulin G (IgG) on neutravidin, where the mass increase was successfully observed in each step (Figure 4A). Similarly, the surface of the cantilever was functionalized with cysteamine, glutaraldehyde, and trypsin while the opposite side was blocked.^[72] Fibronectin concentration was determined by monitoring the surface stress as a function of fibronectin concentration (Figure 4B).

SMR technology was also successfully introduced for detection of unbound molecules, where the targeted biomolecules flow through the cantilever without binding the surface. The mass levels of the particles were quantified from the peak frequency shift. This technology presented an ideal functional assay for predicting the therapeutic response of cancer cells to different drug therapies.^[73] Here, the single cells in suspension repeatedly passed through the fluidic channel around the SMR and were weighed periodically. The mass accumulation rate (MAR) was calculated from the slope of the mass versus time data and mapped over mass. MAR profiles for GBM-PDCLs (patient-derived cell lines), hematopoietic cell lines (L1210 and BaF3-BCR-ABL), and a GBM cell line (U87) were demonstrated. MAR technology was reliable to predict drug susceptibility based on testing with BaF3 cell lines, expressing two subpopulations: wild type BCR-ABL and BCR-ABL T315I, resistant to tyrosine kinase inhibitor, imatinib. Upon the imatinib treatment, BCR-ABL showed significant reduction in their MAR profile while for BCR-ABL T315I cells, no effect was observed.

Recently, a new generation SMR technology was introduced for high-throughput MAR measurements by serially connecting SMRs that are separated by delay channels.^[74] Cells were grown in the delay channels and weighed by each SMR sequentially while other cells could be simultaneously weighed in other SMRs. Therefore, unlike the previous design, there was no limitation to flow only one cell through the SMR at a time, which significantly reduces the throughput. This technology was utilized to assess the therapeutic sensitivity of multiple myeloma cells, a disease that exhibits a variety of cell-based subpopulations to different drug therapies.^[75] MAR response of multiple myeloma cells was studied for different drug therapies and their combinations, that is, dexamethasone (a steroid medication) and bortezomib (a proteasome inhibitor). Therapeutic response of human multiple myeloma cell lines, ANBL-6, expressing wild-type (ANBL-6.WT) and bortezomib-resistant (ANBL-6.BR) subpopulations were studied, where both groups were sensitive to dexamethasone. For the wild type, the reduction in MAR was more pronounced for drugs in combination compared to single drug therapy. On the other hand, for the bortezomib-resistant cell line, MAR reduction was only due to dexamethasone. Other components were also measured for standard-of-care, that is, lenalidomide, an immunomodulatory drug, as well as peptide-based drug targeting E2F/DP1 interaction in combination with extraterminal motif (BET) inhibitor JQ1. MAR assay compatibility was evaluated with clinical samples by performing double-blinded SMR measurements with 12 primary patient samples. Susceptibility and resistance of these patient sample fractions were successfully confirmed with MAR measurements, agreeing well with conventional clinical trials. This technology was also successfully employed to differentiate marine bacteria isolated from their native

environment.^[76] SMR technology is a promising platform for characterizing clonal heterogeneity and predict therapeutic sensitivity of minimal residual disease at single-cell level.^[77] More cellular parameters can be determined by this technology, such as volume and its ratio with mass and density. SMR was used to investigate the origin of the density increase, where the relative density changes of growing yeast cells were measured as the cells are sampled by the microchannel. The state of cell was determined by the direction of the frequency shift in the cantilever response. As shown in Figure 4C, a cell with a density greater than that of fluid appears as a positive mass (negative frequency shift) and a cell with a density less than that of the fluid appears as a negative mass (positive frequency shift).^[78]

Recently, a pedestal mass measurement sensor (PMMS) was demonstrated for adherent cells.^[79] Relation of mass measurement and cell stiffness was determined by measuring the frequency shift by soft and stiff cells (Figure 4D). Quartz crystal microbalance (QCM) platforms were also introduced as an ideal sensor platform to access biophysical properties of cells in a label-free and highly sensitive manner. Commercial QCM sensor, Q-Sense E4 by Q-Sense, Inc., was developed (Figure 4E). QCM sensor consisted of a crystalline quartz disc between two electrodes and when AC voltage was applied, it induced a shear oscillation in the sensor. The resonance frequency of this oscillation was dependent on the total mass. Dissipation of the QCM sensor was also used to investigate cell properties, that is, adherence (soft surface) exhibited higher dissipation while de-adherence (rigid surface) showed low dissipation.^[80]

Another microelectromechanical system (MEMS) was developed to perform multiple clot-time tests for plasma in a single disposable microfluidic cartridge.^[81] Schematic and photograph of the measurement setup comprised an electro-coil for actuating cantilevers, where there was no interconnected electrical components (Figure 4F,G). The functionalized cartridges were performed for real-time coagulation tests. Viscosity and density of the samples were determined based on the variations in the phase of the cantilever vibration response. Independent cartridge and reader unit increased the potential of this approach as a point-of-care system. Time dynamics patterns in the activation of partial thromboplastin and prothrombin were studied in plasma samples from a healthy donor.

A surface stress sensor based on a MEMS design was introduced for label-free biosensing.^[82] The system was based on a Fabry–Perot interferometer that was integrated with a silicon photodiode. The Fabry–Perot interferometer consisted of a thin flexible film and an air gap with a silicon dioxide layer (Figure 4H). The peak position of the transmission spectrum of the Fabry–Perot interferometer was determined by the air gap. Transmission peak value shifted to longer wavelengths when the film deflected due to the presence of the absorbed molecules. In this system, Fabry–Perot interferometer was on top of a photodiode and the sensor was exposed to a single-wavelength light. Therefore, the intensity of the incident light on the photodiode dramatically changed in the presence of a redshift in the transmission response. A detection of 23.7 nA shift was demonstrated in photocurrent at a 3 V reverse bias with immobilized antibodies. A high-Q factor MEMS platform

with a microfluidic chamber was employed for label-free biosensing.^[83] The system employed a microfluidic spray nozzle and microcantilever array (Figure 4I). The solution sprayed onto the cantilever evaporated, leaving residual solutions. A resultant change in the cantilever's mass modified the resonance frequency. Operation of cantilevers in liquid environment exhibited a 50-fold improvement in Q-factor compared to the air, yielding a detection limit of 370 fg.

3. Complementary Devices and Materials

Other contrast generation approaches were realized for field-applicable devices based on electrical, mechanical, and spectroscopic techniques. Some of these nonoptical approaches (particularly electrochemical tools) benefit from low-cost electrical and mechanical components such as current/voltage readers, while other complex designs (for instance, mass analyzers) still require technical solutions to reach highly compact forms. Combining both optical and complementary devices, an all-in-one approach would be transformative for health screening and research purposes by combining both previously described optical devices and nonoptical devices.

3.1. Electrochemical Devices

Electrochemical techniques have received significant attention as they enable miniaturization of biosensors for diagnostic applications. These sensors offer unique advantages for low-cost and easy-to-use portable devices. Their operation principle is based on reacting with an analyte of interest to produce an electrical signal. This signal is then used to determine the presence of the analytes and their concentration with high sensitivity. A typical electrochemical sensor is composed of a working electrode (WE), a reference electrode (RE), and a counter electrode (CE). Electrochemical biosensors could measure potential variations due to the binding of biomolecules that change the charge distribution of the underlying semiconductor material leading a change in conductance, current variations due to the reduction or oxidation of electroactive species, and impedance variations upon immobilization of bilayers at the electrode surface. Electrochemical biosensors lend themselves to portability, owing to their simplicity with low-cost electronics. Their easy-to-use nature could enable real-time detection of the analytes of interest for point-of-care applications.

Recently, a smartphone-based electrochemical impedance spectroscopy (EIS) biosensor system was demonstrated to detect proteins.^[84] The system utilized a biosensor chip, handheld detector, and a smartphone reader (Figure 5A). The electrodes were modified by ligands and protein reactions were measured as electrical impedance signals, which were then transferred to a cell phone by Bluetooth interface. The impedance signals were displayed in the form of Nyquist plot and normalized index was calculated from Nyquist plots of EIS measurement at different BSA (bovine serum albumin) concentrations, where a linear dose-dependent behavior to concentrations of BSA was detected. The system also reliably distinguished different proteins based on the EIS signal. For example, electrodes

were first functionalized with anti-BSA-modified nitrocellulose membranes, then the normalized index values of impedance response showed significantly higher signal for BSA compared to HSA and peptide.

Electrochemical sensors can also be used to detect bacteria from human blood for diagnosis of bloodstream infections.^[85] This portable biosensor utilized a multichannel potentiostat (Figure 5B). Multiplex electrochemical chips were designed on 16 gold electrodes that comprised reference and auxiliary, on which a circular working electrode was coated with a self-assembled monolayer. Each chip was immobilized with target-specific capture probe. The biosensor detected specific 16S sequences of ribosomal RNAs to identify distinct pathogens from samples without preamplification steps. The system exhibited low cross-reactivity with a limit of detection of 290 colony-forming units (CFUs) mL⁻¹ in culture media. To show the potential of the portable biosensor platform, *Enterobacteriaceae* positive blood cultures that consisted of *Enteric bacteria* (EB), *Escherichia coli* (EC), *Proteus mirabilis* (PM), and universal (UNI) probes. Current values for EB detection diagnosed samples as positive for EC and negative for PM, demonstrating that the platform can successfully identify pathogens in blood.

Paper-based microfluidic platforms can be integrated to electrochemical readout devices to achieve sensitive and low-cost sensors. A paper-based electrochemical sensor was realized for multiplexed detection of biomarkers in such a microfluidic interface.^[86] The system utilized eight electrode-sensors for simultaneous detection of different analytes that were connected to a handheld potentiostat for electrochemical signal readout (Figure 5C). To show its multiplexing capability, paper chip was divided into three channels to detect glucose, lactate, and uric acid in urine. Chronoamperometric curves showed a linear relationship for various uric acid concentrations as a function of current. LOD values were comparable to commercial paper-based platforms, that is, 0.35, 1.76, and 0.52×10^{-3} M for glucose, lactate, and uric acid, respectively.

Electrochemical techniques could also enable wearable sensing technologies. A label-free cortisol biosensor was integrated to a nanoporous flexible electrode system for field applications.^[87] The wearable device was implemented as a disposable sensor interface on user's skin (Figure 5D), utilizing reference and working electrodes within the polyamide membrane. The system achieved low sensing volume (1–5 μ L) through a sensor design that was composed of vertically aligned metal electrodes with semiconductive MoS₂ nanosheets, which were functionalized with antibodies to attach cortisols on the electrode surface. The system showed a LOD within the physiological relevant range of cortisol in human sweat, in which blue line corresponded to the cortisol calibration.

Commercial portable electrochemical sensors were also developed for point-of-care applications. For example, i-STAT handheld sensor by Abbott Laboratories comprised a handheld analyzer and a disposable cartridge (Figure 5E). The cartridge contained calibrant solution and conductivity pads to make electrical contact with an analyzer, and a series of biosensors were composed of thin metal film electrodes. The blood sample was loaded to the cartridge with a capillary tube. The resultant signal from the electrochemical biosensors in response to the calibrant solution was transmitted from contact pads to the

analyzer. Electrical signal of the test and calibration samples were compared to determine the concentration of the samples. The system provided fast, accurate, and reliable sensing results. Another commercial handheld electrochemical biosensor was EmStat Blue by PalmSens, a small USB and battery powered potentiostat that was interfaced to a Bluetooth communication unit. This handheld biosensor utilized cost-effective and screen-printed carbon electrodes for ease of use (Figure 5F). The electrodes of this portable device worked with droplets of the targeted samples, providing a very simple and convenient way of analyses.

Electrochemical biosensors were used to screen anticancer drugs through the analysis of DNA damage on molecular compositions.^[88] The effect of the paraben-based cyclotriphosphazene compounds was investigated on DNA using a new electrochemical biosensor, which was called MiSens (Figure 5G). Compared to conventional genotoxicity testing techniques, this system provided quick and inexpensive monitoring of drug and DNA interactions. The platform was based on real-time electrochemical profiling (REP) technology for investigation of the genotoxicity by measuring the DNA hybridization efficiency on the biochip surface. DNA hybridization was achieved through an immobilized capture probe, a hybridized target, and a detection probe. Hybridized target and detection probe solution were incubated in a paraben solution, followed by capturing of probes to assess the hybridization of the target to its complementary surface probes. During the real-time electrochemical profiling, the DNA damage reduced the electrical signal while the DNA target with no damage increased the current (Figure 5G).

3.2. Mass Spectrometry Devices

A unique multiplexed detection device is mass spectrometry, a ubiquitous technology for drug screening and clinical applications.^[89] This method identifies chemical species and ions based on the mass-to-charge ratio. Pure materials and complex samples have widely been processed by mass spectrometers for industrial and academic applications. The sample of interest is vaporized and then subjected to a mass analyzer for identification of individual elemental compositions. While many mass spectrometer components are sophisticated and costly, there have been extensive efforts in miniaturization of mass detection devices for field applications. Design requirements of a portable mass spectrometry rely on atmospheric compatibility and vaporization of samples (both volatile and non-volatile) in ambient conditions.^[90]

Early handheld demonstration of a mass spectrometer design was Mini 10, a rectilinear ion trap method.^[91] This device was in the size of a shoebox (32 cm \times 22 cm \times 19 cm) and 10 kg total weight (Figure 6A). Based on a power consumption level that was less than a laptop, this portable mass spectrometer allowed multiplexed chemical detection of toxic substances such as *n*-butylbenzene, methyl salicylate, and 1,3-dichlorobenzene in air and naphthalene in water with a 50 ppb detection limit. Former miniaturized mass spectrometers had required active pumping system to enable vacuum for ionization, while an ambient (room condition) ionization was preferred in the later designs.

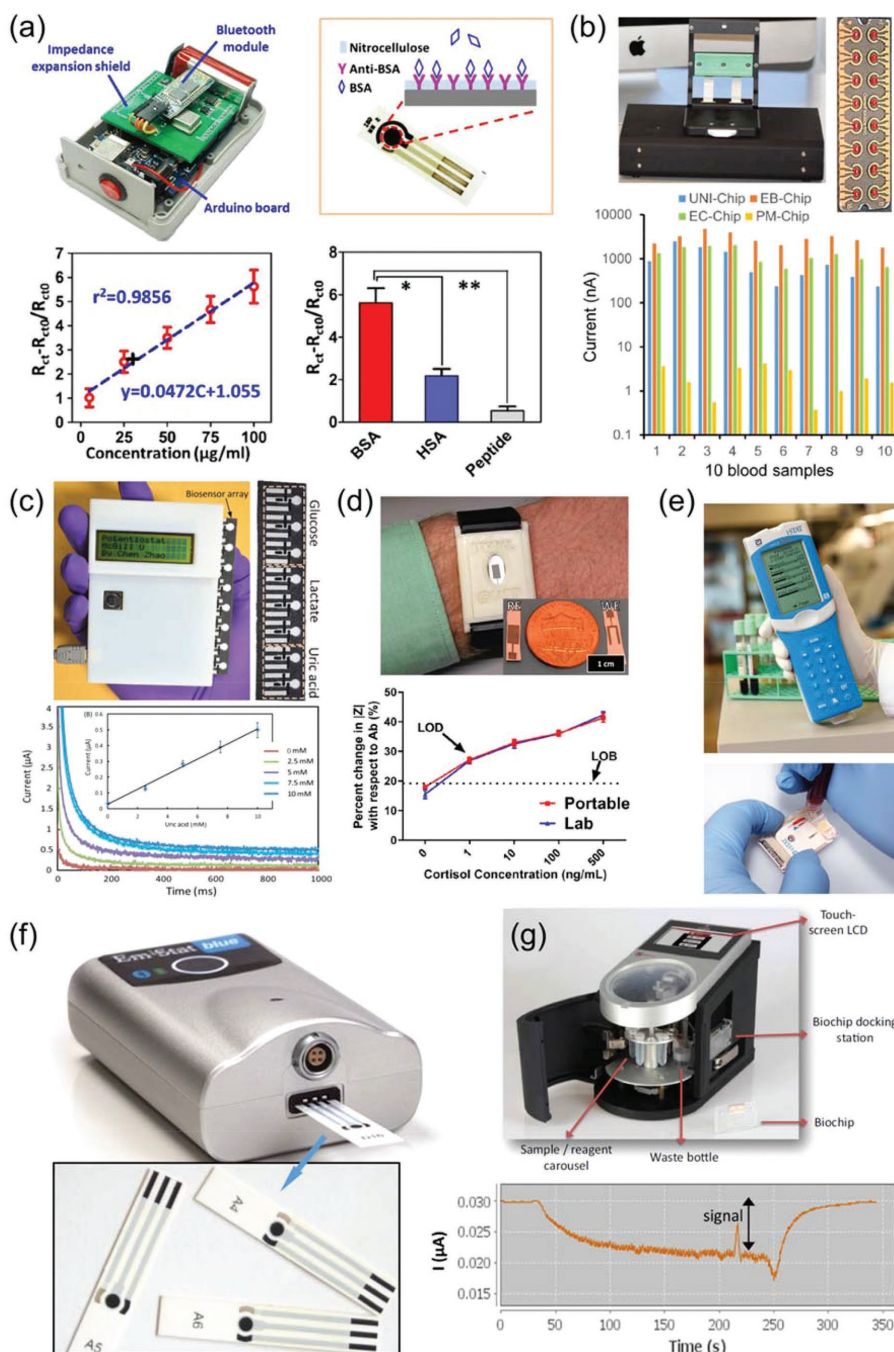


Figure 5. Electrochemical devices. a) Top left: Photo of inner components of the handheld electrochemical biosensor. Top right: Electrode modified by anti-BSA with nitrocellulose membrane. Bottom left: BSA concentration – EIS signal correlation (EIS = electrochemical impedance spectroscopy). In the figure, R_{ct0} is the initial charge transfer function (R_{ct}). Bottom right: EIS signal for BSA, has, and peptide. b) Top left: Portable electrochemical biosensor based on multichannel potentiostat. Top-right: Biochip with 16 sensors, consisting of a central working electrode, a circumferential reference electrode, and a short auxiliary electrode. Bottom: Current outputs of different sensor chips for a blood sample with *Enteric bacteria* (EB) positive. c) Top left: Photograph of the paper-based biosensor with a potentiostat. Top right: Paper-based electrode sensor array. Chronoamperometric (bottom) and calibration (inset) curves for uric acid. d) Top: Wearable electrochemical biosensor for cortisol detection from human sweat. Inset: close-up of the sensor. Bottom: Calibration curve: percent change in impedance versus cortisol concentration. e) i-STAT handheld sensor by Abbott Laboratories (Reproduced with permission from <https://www.pointofcare.abbott>). f) EmStat Blue by PalmSens (Reproduced with permission from <https://www.palmsens.com/product/emstat/>). g) Top: MiSens biosensor. Bottom: Real-time DNA profiling by monitoring current signal. High signal: No DNA damage. Reduced signal: DNA damage. Reprinted from refs. [84] (a), [85] (b), [86] (c), [87] (d), and [88] (g) with permission: Copyright 2015 and 2017, Elsevier B.V. (a and g); Copyright 2016, Society for Laboratory Automation and Screening (b); CC-BY-NC-SA 3.0 open access publication (c), CC-BY 4.0 open access publication (d).

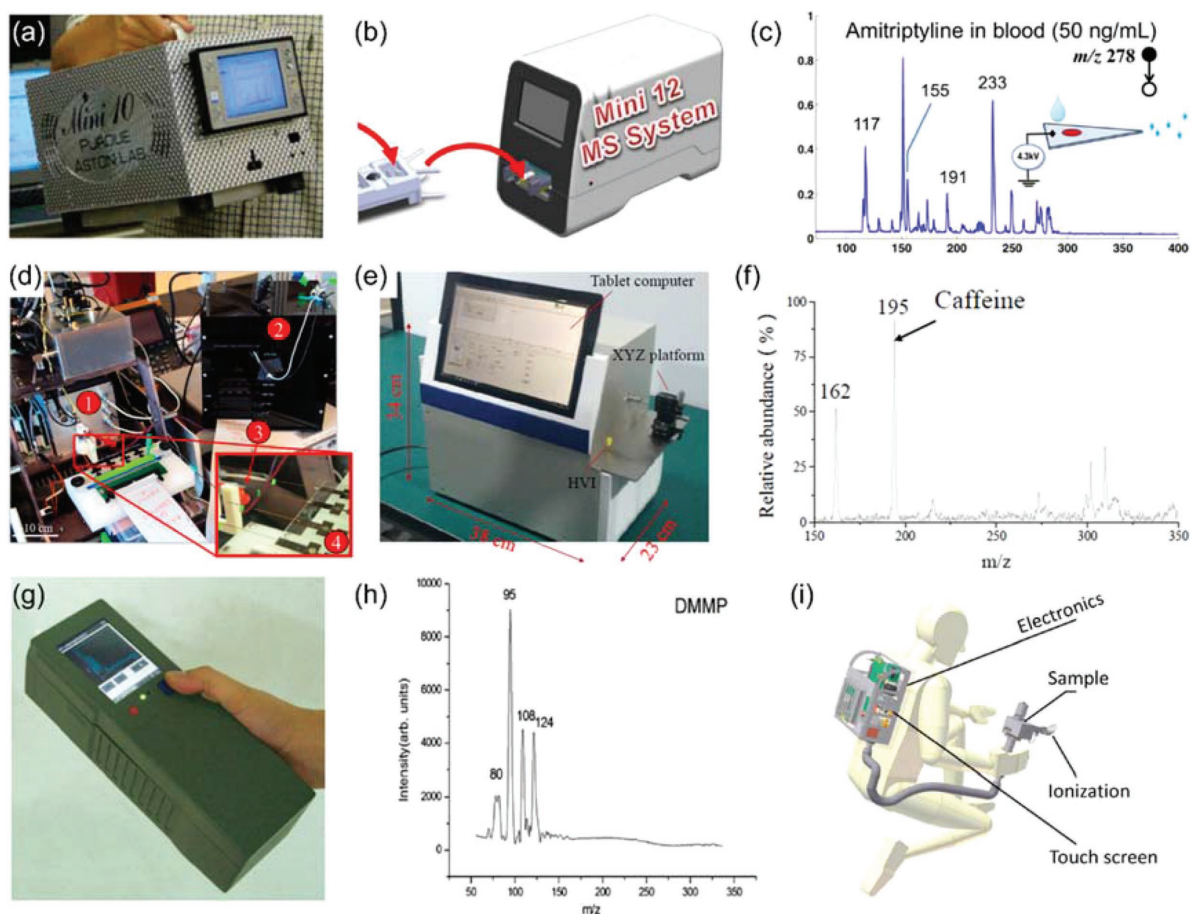


Figure 6. Mass spectrometers. a) Handheld mass spectrometer, Mini 10, with rectilinear ion trap design. b) Another implementation of portable mass spectrometer with ambient ionization, an advancement for field applications. c) Mini 12 quantified drugs (Amitriptyline) in blood samples for diagnostics. d) An automated sample preparation by digital microfluidics (denoted as 2–4 components) combined with Mini 12 (denoted as 1 component) for quantification of drugs of abuse. e) An alternative Mini 2000 mass spectrometer based on continuous atmospheric pressure interface. f) Chemicals were identified by Mini 2000, including a caffeine sample at 195 m/z . g) A palm mass spectrometer was developed for particularly chemical warfare agents in field settings. h) An organic gas (dimethyl methylphosphonate) was measured by a palm portable mass spectrometer. i) A backpack design for a wearable mass spectrometer toward real-time chemical agent detection on surfaces. Reprinted from refs. [91] (a), [92] (b), [93] (c), [95] (d), [97] (e,f), and [98] (g,h) with permission: Copyright 2006 and 2014, American Chemical Society (a,d,i); ACS AuthorChoice License open access publication (b,c); CC-BY 4.0 open access publications (e,f); Elsevier user license open access publication (g,h).

Despite increasing the size and complexity of devices, Mini 12 (a recent implementation of mass spectrometers) provided chemical detection with minimal sample preparation and automated analysis (Figure 6B).^[92] Mini 12 platform analyzed therapeutic drugs such as amitriptyline, amitriptyline-d6, and thiabendazole in blood samples with 7.5 ng mL⁻¹ detection limit (Figure 6C).

Another significant advance is to combine automated sample preparation by microfluidics, followed by chemical analyses based on miniaturized mass spectrometers. Mini 12 analyzed samples that were prepared by a digital microfluidic platform to electrostatically handle liquids with an array of electrodes (Figure 6D).^[93] Using this integrated platform, a wide range of drugs including cocaine, benzoylecgonine, and codeine were prepared in 15 min as a dried form and these target specimens were measured up to 40 ng mL⁻¹ sensitivity.

An alternative mass spectrometry approach is to use atmospheric pressure. Using this method, A Mini 2000 platform was developed and integrated with a handheld tablet computer

(Figure 6E).^[94,95] This miniaturized mass analyzer measured caffeine and other polyethylene glycol (PEG) 600–1500 chemicals at specific alternating current injection frequencies up to 10 ng mL⁻¹ sensitivity (Figure 6F). Integration of a lightweight tablet computer alleviated the need for a standalone notebook/desktop computer, providing ease-of-use for field applications. Additional miniaturized mass spectrometers using ion funnels increased the efficiency of chemical identification.^[96] Most of these compact units, including Mini 10-12 systems, Mini 2000 device, and ion funnel approach, were designed for minimally trained personnel, making them ideal for portability and robustness for diagnostics and experiments.

Palm portable mass spectrometer (PPMS) was the most compact form of chemical analyzers (Figure 6G).^[97] PPMS utilized a battery-powered circuit to drive an ion trap assembly for mass analyses. While size reduction in the device design influenced ion efficiency, the PPMS device measured toluene up to 5 ppm and dimethyl methylphosphonate (DMMP) up

to 22 ppm (Figure 6H). In addition to portability, a backpack design was also demonstrated for on-site monitoring of toxic substances in point-of-care conditions (Figure 6I).^[98] This wearable device utilized a low-temperature plasma probe to measure nonvolatile components on active surfaces, providing numerous opportunities for chemical analyses by mass analyzers in field settings and even in space.^[99]

Another recent implementation of mass-based chemical analysis allowed diagnosis of cancerous and normal tissues by a handheld probe (MassSpec Pen) that was connected to a commercial Orbitrap mass spectrometer.^[100] Using this benchtop platform, tissue samples from 253 human subjects were analyzed and accurately classified based on cancer types. Other commercial mass spectrometers such as Micromass Quattro Ultima mass spectrometer were also used to test oral fluids for drug substances such as cocaine and benzoyllecgonine.^[101] Current development efforts of miniaturized mass spectrometers in both academic laboratories and companies continue to provide highly multiplexed identification of chemicals in bodily fluids and environmental samples.

4. Applications in Field Research and Diagnostics

4.1. Global Health

Medical practice in the developing parts of the world is limited to a handful of basic diagnostic and testing devices.^[102–104] Advanced equipment is not affordable in these low-resource settings. These countries also experience high prevalence of life-threatening infectious diseases. The presented portable diagnostic devices offer solutions to this important need. Particularly, smartphone penetration to resource-limited countries is significant, allowing clinical testing in field settings. To this end, a mobile phone based microscope was used to diagnose malaria, a major global health challenge (Figure 7A).^[105] In this design, polarization light microscopy on the cellphone camera unit allowed detection of malaria-infected regions of tissues based on imaging of hemozoin, a malaria pigment. Another platform was developed for *Schistosoma haematobium* infections in rural Ghanaian schools.^[106] A library of 60 patient samples from randomly selected students was screened by mobile phone diagnostics with 72.1% sensitivity. This device can be used for multiplexed analysis of infected samples based on bright-field contrast changes.

Another platform was a smartphone microscope (CellScope) that measured *Filarial* parasites in whole blood by digital enhanced cellphone video frames (Figure 7B).^[107] This portable mobile detector measured blood samples from 33 *Loa*-infected patients in Cameroon with 94% specificity and 100% sensitivity. An advance to this CellScope design was to combine multicontrast imaging (dark field, bright field, and phase imaging) in the same platform for multiplex field applications.^[108]

An alternative approach was the integration of microfluidic sample preparation unit with multiplexed smartphone imaging (Figure 7C).^[5] This smartphone dongle (powered by the audio jack) was then used to test 96 patients for simultaneous screening of HIV, treponemal syphilis, and nontreponemal

syphilis (three markers with positive and negative controls) in Rwanda with 90–100% specificity in blood samples. Portable, handheld, and miniaturized devices will continue impacting global health challenges with enhanced multiplexing capabilities.

4.2. Personalized Monitoring

Although developed countries have access to adequate medical facilities, the frequency of medical testing is still limited to medical infrastructures. The delays in health screening of individuals cause a cost-burden and decrease quality of life. As a key solution to enhance patients' medical testing in homes and public venue, on-site analysis of biomarkers by portable and multiplexed devices could enable personalized screening of health in remote settings. Rapid results from diagnostic tests near patient's native environment allow early detection of abnormal signs toward cancer screening. Continuous acquisition of disease symptoms by mobile devices can serve as a health management platform. In particular, mobile phone based diagnostic and analysis provide much-needed tools for personalized medicine.^[109]

To this end, an integrated home-based semen analysis device was developed for male infertility evaluation using microfluidics, optical imaging, and smartphone readout (Figure 7D).^[110] This portable device was validated in 350 clinical samples by screening concentration and mobility of sperms in less than 5 s of processing time. The device attachment utilized low-cost white LED, two aspheric lenses, and electrical components. The reliability of testing results of this smartphone analyzer was compared to a computer-assisted semen analysis (CASA), yielding 98% accuracy. The results from untrained users and trained personnel were not different, exhibiting low mean errors with statistically insignificance for the semen samples from all the patients. This smartphone-based semen analyzer provided a personalized infertility diagnostics platform for home use and even broadly applicable to remote clinics.

Another personalized diagnostic platform was albumin detection in urine by a smartphone reader (Figure 7E).^[111] This portable tool was developed to frequently measure the blood proteins that leak into the urine samples due to the kidney damage in chronic patients such as diabetic individuals. The device was an integration of low-cost laser diode, disposable tubes, batteries, and a plastic lens. The analysis of spiked albumin in synthetic urine samples yielded 5–10 $\mu\text{g mL}^{-1}$ sensitivity that was threefold lower than the clinical range of albumin in urine specimen from patients. This smartphone-based urine analyzer took 5 min to obtain the test results in home settings, providing an automated solution for early diagnosis of kidney diseases.

In addition to these advances, commercial portable readers were used for personalized monitoring of a range of physiological parameters, including pressure and glucose analysis in blood, body physical metrics such as weight and ratios, as well as sleeping and physical patterns.^[112] A recent demonstration was the analysis of 250 000 daily physiological measurements from 43 individuals using wearable biosensors, a combination of heart rate measurements, skin temperature

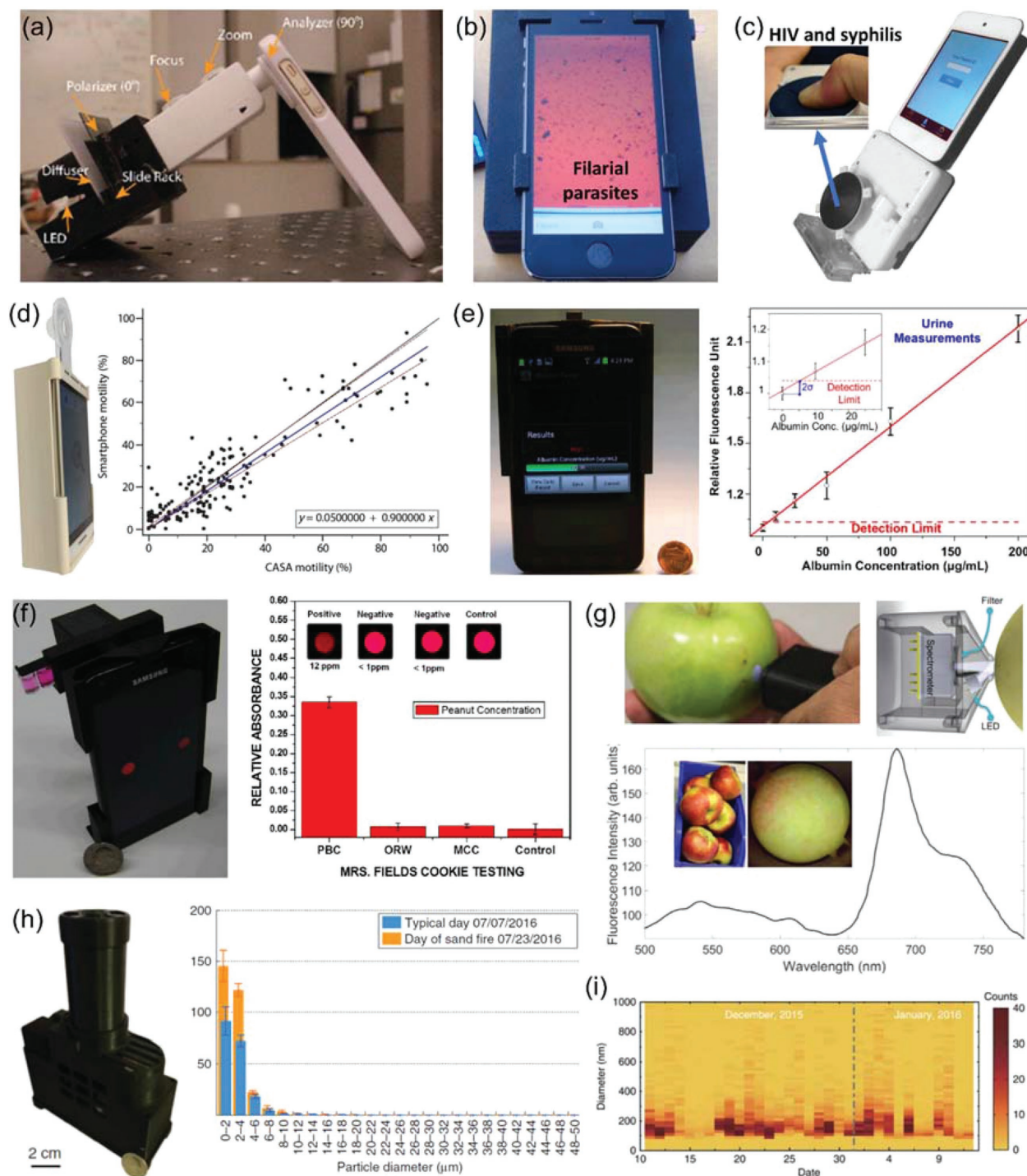


Figure 7. Applications of field portable devices. a) Mobile phone polarized microscope for *Malaria* diagnosis. b) Multimodal CellScope for detection of *Filarial* parasites in whole blood. c) Smartphone dongle for multiplexed detection of HIV and *Syphilis* in Rwanda. d) Automated semen analysis by a microfluidics and smartphone reader for home-based male infertility diagnostics. e) Albumin testing in urine by fluorescent assays and smartphone imaging for frequent kidney monitoring. f) Left: Cell phone-based allergen testing platform. Right: Peanut concentrations determined from three different cookies: peanut butter chocolate (PBC), oatmeal raisin with walnut (ORW), and milk chocolate chip (MCC), tested by the handheld allergen testing platform. g) Spectroscopic analysis of fruits by a handheld analyzer integrated with smartphones. Upper left: Process of spectral data acquisition, upper right: the nozzle opening at an angle to the spectrometer, bottom: fluorescence spectrum for McIntosh apple. h) Left: Real picture of the handheld particulate matter (PM) testing platform. Right: Histogram of the PM data for a regular day and a day of sand fire in Los Angeles, measured from the same location. i) PM data (size distribution) in Beijing atmosphere from December 11, 2015 to January 12, 2016 monitored by the air quality analyzer with nanofibers. Reprinted from refs. [105] (a), [107] (b), [5] (c), [110] (d), [111] (e), [119] (f), [120] (g), [127] (h), and [128] (i) with permission: CC-BY 4.0 open access publication (a,g,i); Copyright 2015 and 2017, American Association for the Advancement of Science (b,c,d); Copyright 2001 and 2012, Royal Society of Chemistry (e,f); Copyright 2017, Springer Nature (h).

recordings, blood oxygen quantification, and physical activity mapping.^[113] This personalized platform revealed physiological variations of diabetic patient subtypes, blood oxygen fluctuations during high-altitude flights, as well as early signs of Lyme disease. Another comprehensive personalized health management platform was a wellness study of 108 individuals based on large-scale omics (genome to metabolite) profiling together with physical activity.^[114] Molecular analyses and personalized data allowed early identification of diseased formation. The presented optical multiplex devices, when combined with such large-scale studies, could improve life quality of individuals in a precise and timely manner.

4.3. Food and Nutritional Testing

Portable devices could also significantly improve public health by monitoring the ingredients in food products, particularly allergens. The current methods to detect hidden allergens in food products include surface plasmon resonance,^[115] electrochemical immunosensors,^[116] PCR,^[117] and mass spectrometry.^[118] Despite their high sensitivities, these conventional techniques are complex and need bulky equipment. Therefore, there is a strong need for affordable and easy-to-use sensing platforms for personal use. Recently, a food allergen testing platform was integrated to a cell phone to perform colorimetric assay analyses.^[119] Portable allergen testing platform included test and control tubes inserted from the side and illuminated by two LEDs (Figure 7F). The allergen assays in the tubes absorbed light, resulting in intensity change acquired by the cell phone camera. The images can be digitally processed in 1 s for detection and quantification of the allergens. The calibration curve was measured from different peanut allergen concentrations and then converted into absorbance values, yielding a minimum detectable peanut concentration as low as ≈ 1 ppm. Peanut values in peanut butter chocolate (PBC), oatmeal raisin with walnut (ORW), and milk chocolate chip (MCC) cookies were measured, where the peanut content in PBC was successfully determined, while ORW and MCC show negligible absorbance signal change in the control level. This smartphone-based testing platform could be applied to other allergens to significantly improve the quality of life of individuals allergic to different food products.

A smartphone-based spectrometer was demonstrated as a wireless connected and standalone platform. The device was low-cost and the power consumption was minimal making it portable, a critical need for applications in field settings.^[120] The device consisted of a spectrometer chip, white or UV LED, optical filters, a Bluetooth module, a microcontroller, and a rechargeable Li-ion battery. Photograph of the process of spectral data acquisition was shown in Figure 7G. In the device, the LED was arranged in the vicinity of the nozzle opening at an angle to the spectrometer allowing efficient illumination. The handheld platform determined UV fluorescence of chlorophyll (ChlF) found in plant-based components like fruits. ChlF exhibited a positive correlation with the ripeness of the fruits. ChlF detection tests were performed with variety of apple (*Malus domestica*) samples. Ripeness estimation was carried out using mechanical firmness testing and the data were compared with

ChlF measured with the portable device. Typical fluorescence signal for McIntosh apples exhibited low fluorescence values in the 500–600 nm wavelength range, yielding similar values to the case of green apples.

Portable devices can also be used to determine food deficiency. For instance, ironPhone was coupled to point-of-care testing for assessment of iron status, an urgent public health problem related to maternal and child health.^[121,122] The device assessed the iron status based on serum ferritin levels. The platform showed a positive correlation with the standard lab analyses with a sensitivity of over 90% for predicting iron deficiency. Another phone-based low-cost device was introduced for determining vitamin B₁₂ deficiency that is necessary for formation of red blood cells, DNA synthesis, neural myelination, brain development, and growth.^[123] The platform utilized a lateral flow assay with necessary reagents and built-in flow control. The system used a finger-stick of blood for test and B₁₂ test strips were imaged with smartphone platform, where the images were processed with the smartphone app for quantitative analyses. Human trials were successfully performed for blood vitamin B₁₂ status from an $\approx 40 \mu\text{L}$ finger prick blood of 12 participants.

4.4. Air Monitoring

Portable sensor platforms could also improve the quality of life by monitoring the air pollution in real time. Particulate matter (PM) determines the air quality and main source of high number of PM is power plants, industrial infrastructure, automobiles, or fire. PM monitoring is performed by air sampling stations, employing beta-attenuation monitoring or tapered element oscillating microbalance instrument.^[124] These methods are accurate and can produce high-throughput PM data. However, these devices are bulky, high cost, and need experienced professionals. To address the need for portable PM testing platforms, commercial devices were developed, that is, Fluke 985 indoor air quality particle counter and 10 TSI Model 3007 handheld particle counter. However, these devices exhibited low sampling rate and dynamic range, conversion problems between measured light intensities and actual particle size. Accurate sample size data could be enabled by microscopy techniques.^[125,126] However, these techniques needed separate measurement and analysis, significantly extending the result preparation duration. These devices were also expensive as the image data need to be evaluated by an expert in a central lab and were not compatible with field applications due to their bulky setup. To address this need, a handheld PM testing platform was introduced to determine the automated size information and high-throughput quantification of particle sizes.^[127] The system uniquely combined lens-free microscopy and machine learning for PM quantification. As shown in Figure 7H, the sample was positioned on top of the imager. The platform employed a micro-pump, air sampler, and a lens-free microscope. The system also utilized a machine learning algorithm for PM data process. In the platform, the aerosol samples were captured by a sticky coverslip cast in-line holograms, which were then recorded for reconstruction and further processing to determine the PM statistics. The system monitored 6.5 L of air in 30 s and real-time provide

PM information with 93% accuracy. PM data comparison between a regular day and a sand fire in Los Angeles showed an enhancement in the number of particles in the sand fire.

Recently, a portable, real-time, and ultrasensitive spectrometer was demonstrated with a size resolution of 10 nm for detecting 100 nm diameter nanoparticles for air quality monitoring.^[128] A waveguide structure that comprised of five nanofibers was used with a long joint fiber loop to minimize the polarization change and to increase the sensing area. A syringe pump was utilized to inject the nanoparticles into a gas pipe and then to the nano-waveguides via the glass nozzle. A 680 nm diode laser and a photodetector allowed monitoring the transmitted power in real time. A polarization controlling system was used to generate a circular polarized probe light. Circular polarized light enabled a scattering efficiency induced by a nanoparticle in the vicinity of the nano-waveguide independent of the binding position. Size distribution of the particles from December 11, 2015 to January 12, 2016 was presented (Figure 7I). The trend was consistent with the official PM data that were reported by the Beijing Municipal Environmental Monitoring Center.

4.5. Other Applications in Extreme Conditions

Biological warfare agents need to be detected as early as possible during an attack.^[129] Multiplex biosensors were employed to target viruses and bacteria from a sample in battlefield settings.^[130] Commercial bead assays detected four distinct targets that comprise the RNA bacteriophage (MS2), *ovalbumin* (Ov), *Bacillus globigii* (Bg), and *Erwinia herbicola* (Eh) with a few $\mu\text{g mL}^{-1}$ sensitivity in less than 30 min of assay time.^[131] In parallel, miniature mass spectrometers were designed to detect toxic substances in the circulating air of a war zone.^[97,98] Comprehensive biosensors are now being developed to cover a wide range of chemical threat agents using a combination of antibodies, lectins, nucleic acid probes, aptamers, whole cells, and bacteriophages.^[132]

Field monitoring of crew team, spacecraft machine, and environmental health necessitates point-of-care devices.^[133] These measurements in space conditions allow exploration of harsh atmospheric conditions and gravity on biological and chemical systems. Molecular level imaging in cells was also studied for space applications by changing microgravity.^[134] Miniaturization efforts in multimodal microscopy design impacted study of microorganisms in space.^[135] Multiplex portable devices will be highly valuable for investigating the properties of biological systems in space as well as investigating the potential signatures of extraterrestrial life.

5. Analysis and Data Handling from Devices

Multiplex devices generate unprecedented data from diagnostic and research specimens. This digital complexity is either stored and processed in the portable device, or alternatively, categorized information is distributed to a central processor through a series of connection methods. Recent advances in computation (for instance, machine learning) are then employed to

make sense of the digital results. While the analysis of assays from a single device is rather useful, accumulation of digital knowledge from multiple devices can be more informative of disease progression and underlying mechanisms (Figure 8). Multiuser (patients, researchers, and experts) operation of decision-making process in health-related data necessitates accurate information processing of diagnostic results. Untrained and trained personnel should be involved within a reasonable time frame, yielding early detection capabilities and accurate determination of indicative markers.

5.1. Connectivity and Network

Portable devices typically report levels of diagnosis in field conditions without direct involvement of medical personnel. The computer processors in standalone devices and smartphones provide sufficient speed and storage for individualized tests. Portable devices implemented directly on smartphones already benefit from advanced digital power embedded in the high-end microprocessors of phone circuitry. On the other hand, to enhance capabilities of separate handheld units and low-end cellphones, a wireless or Bluetooth communication^[136–141] is preferred to transfer the health-related data to smart device interfaces (smartphones or tablets) or a central analysis software running on off-site computers.^[142] Regardless of the choice of connectivity method, the end user reaches the convenient diagnostic test results from personalized viewers on phones or device monitors.

However, the accuracy of these personalized testing is still questioned. Thus, test results are perceived as an indicator, but not a complete diagnosis. To obtain recommendation of a health decision maker, diagnostic data are then transferred to a physician or medical expert. In a recent study, test results from anticoagulation, diabetes, urinary tract infections, strep throat bacterial test, influenza, pregnancy, anemia, infectious mononucleosis, acute cardiac conditions, and lipid problems were presented to primary care physicians on a weekly basis.^[143] Out of 317 participants in developed nations, 38% (120 physicians) identified satisfactory benefits of point-of-care, while 27% exhibited concerns of diagnostic precision. Patient and medical doctor network in personalized monitoring applications by portable and multiplex devices were mostly perceived as a positive experience.

For global health needs, point-of-care multiplex devices are deployed in remote primary healthcare clinics in especially rural locations. In this context, the test data should only be transmitted between medical professionals. To assess efficacy of portable devices, a pilot study was performed in KwaZulu-Natal, South Africa.^[144] Point-of-care tests were handled by the professional healthcare workers instead of end users. In 100 rural clinics, creatinine (37%), tuberculosis (31%), CD4 count (37%), cholesterol (32%), and HIV viral load (23%) were the regularly used portable tests, among many others. Even some of the experienced nurses failed to provide accurate referrals based on diagnostic tests. Therefore, portable and multiplex diagnostic tests should still be administered by proper training in these low-resource settings to enable accurate diagnosis.

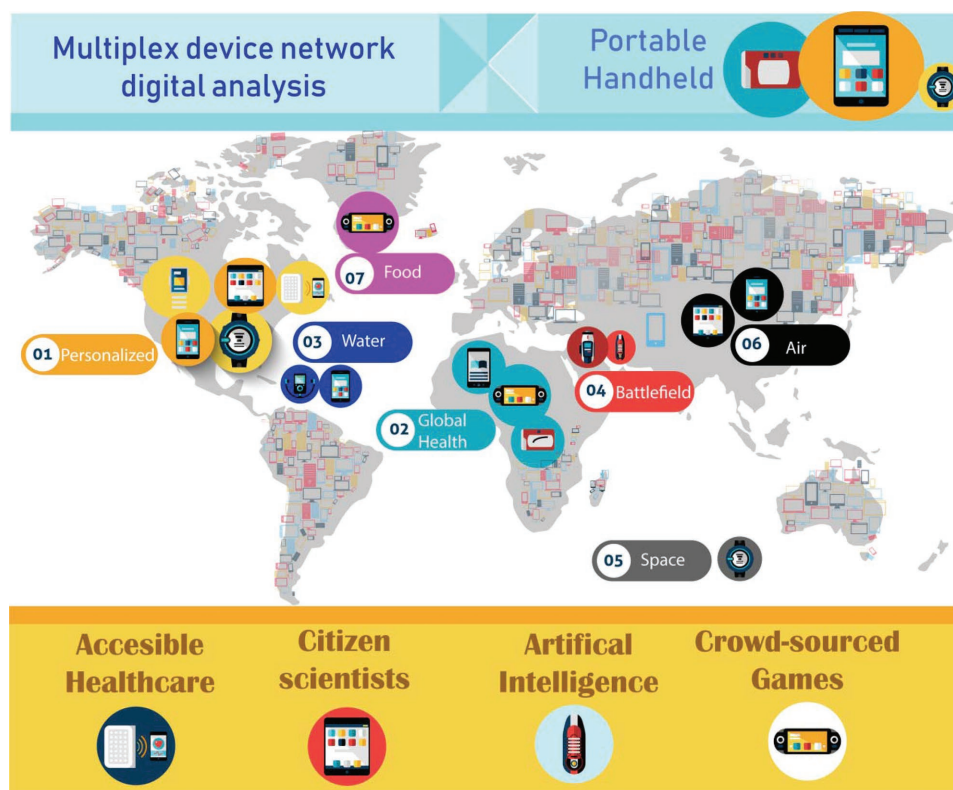


Figure 8. Worldwide distribution, connectivity, and analysis of multiplex assays and technologies. Personalized monitoring, global healthcare, battlefield diagnostics, water and air quality screening, food testing, and space research applications utilize large-scale and digitally connected network of portable devices. These global solutions improve healthcare delivery, stimulate emergence of citizen scientists, leverage specialized artificial intelligence for robustness, and enhance social networks through entertainment such as crowd-sourced games.

Testing data from multiplex devices can also be transferred to a central server toward the development of a global health management platform (Figure 8). A recent approach was a spatiotemporal mapping of rapid diagnostic tests that were analyzed by a smartphone reader.^[31] Test results (with original images) from lateral flow assays (specific to malaria, tuberculosis, and HIV) were transmitted to a central server along with corresponding geographical position and patient-related data. Combining diagnostic data from different parts of the world on a web interface allowed real-time monitoring of infectious disease epidemics. This spatiotemporal disease management concept was then adapted by multiplex diagnostic assays running on smartphones that targeted Zika viruses in urine and saliva.^[145]

Transmission of on-site diagnostic data to main servers experiences a patient privacy concern. During the migration of the data and access to the online database, information about patients should remain confidential. A direct solution is to keep password-protected web interfaces.^[31] Additional precautions have already been designed by encrypting and scrambling the patient data by signal processing approaches.^[146] Portable devices digitally distribute the information, making the sensitive patient data vulnerable. To avoid any complications with patient privacy, regulatory measures from the Food and Drug Administration (FDA) should be met to comply with the “mobile medical application policy.”^[147]

5.2. Analysis Methods

Quantification of multiplexed portable devices is mostly performed based on analytical characterization in the spectral features and spatial imaging data.^[148] Particularly, optical devices utilize light transmission,^[149] absorption,^[150] fluorescence,^[151] colorimetric,^[152,153] and luminescence.^[154] Each mechanism uses light enhancement/reduction calculations in portable devices. Initial step for multiplex assays is to validate detection of analytes using a wide range of concentration samples, followed by a point-of-care testing of the target specimens. To address accuracy concerns of medical experts, repeatability and robustness of the multiplexed detection device should be accurately established.^[155–157] The detection limit of these portable devices should also meet the clinically accepted ranges.^[130,158]

Digital assays were also pivotal in point-of-care device design.^[159] Instead of measuring signal change in the total sample volume, target samples were distributed into thousands of smaller volumetric partitions. The signal readout from each subvolume was then amplified to have either positive or negative output. Counting the number of positive partitions then provided the concentration of target analytes based on the Poisson statistics with adequate data points. For instance, a room temperature PCR was performed in a microfluidic chip (SlipChip) that splits samples into multivolumes (160 wells with 1–125 nL capacity) for quantification of viral HIV and hepatitis

C (HCV) RNA targets.^[151,152] Multiplex detection achieved a dynamic range of 10^2 – 10^7 molecules mL^{-1} at threefold resolution. Results from digital analyses were validated by Roche COBAS AmpliPrep/COBAS TaqMan HIV-1 Test.^[159–161]

Machine learning (broadly known as artificial intelligence, AI) has received considerable attention for medical predictions from patient-related data.^[162] For instance, intricate differences of cell types in blood specimens were accurately identified based on machine learning and its specific implementation of deep learning.^[163,164] For field applications, the performance metrics of portable devices do not match the quality of the benchtop counterparts. Thus, learning algorithms make up for the imperfections in the low-cost optical design to enhance the repeatability of multiplexed detection results. Another benefit of machine learning based analysis is the iterative and adaptive correction of target detection based on accumulation of large-scale data from portable devices. As a demonstration to this algorithmic approach, recently waterborne parasites were imaged by a mobile phone fluorescent microscope and the captured cysts were sensitively quantified by a custom machine learning framework.^[165] A library of 71 features in the cyst candidates were trained by the algorithm in 1370 cyst images and 1485 other particles to identify true signal for a parasite and exclude unwanted signatures. Another application of learning algorithms was microparticle detection for air monitoring.^[127] Machine learning analysis accurately predicted the size (diameter) range of the microparticles based on spatial and intensity features in images from the portable device. Deep learning (a particular implementation of machine learning) was also used to enhance microscopic analysis platforms running on smart phones and field-portable imagers.^[166,167] Artificial intelligence algorithms will continue transforming the sensitivity, specificity, and robustness of portable multiplex devices, providing a smart software solution for the global health issues.

Global health management platforms (connected portable devices on a web server) utilize crowd-sourced based health data.^[168] Previously, crowd-sourced search engine results were used to predict influenza epidemics worldwide, followed by statistical analysis and predictions.^[169,170] Similar to these initiatives, results from distinct users of multiplex assays were interpreted based on mathematical and computational frameworks. For instance, smart phone voice recordings of mosquitos were classified by maximum likelihood estimation (MLE) of wingbeat frequencies.^[7] Another recent work combined entertaining games with crowd-sourcing (BioGames) to diagnose malaria from microscopic pictures.^[171,172] An analogy of telecommunication theory was used to compute a maximum a posteriori probability (MAP) for estimation of malaria-infected red blood cells. Citizen scientists globally enable large-scale biological discoveries through games, field experimentation, and digital analysis.^[173]

6. Multiplex Assays and Devices Market

The global multiplexed diagnostic device market was valued \$8.43 Bn in 2016 and is projected to increase to \$17.85 Bn by 2025 with a compound annual growth rate (CAGR) of

9.4%. However, conservative figures indicated a CAGR of 7.5%.^[174,175] As of 2017, the North America held 56.3% of the global multiplexed diagnostic device market, and Asia pacific is expected to grow at the highest CAGR (22.5%) until 2025.^[176,177] The key players in multiplexed devices market include Abbott Laboratories, Thermo Fisher Scientific, Merck Millipore, Bio-Rad Laboratories, F. Hoffmann-La Roche, Cepheid, Qiagen, and Luminex Corporation. The global multiplexed diagnostics market is dominated by Thermo Fisher, Abbott, and Agilent that had a combined market share of 59.5% in 2015.^[178] The largest segment of multiplexed diagnostics market is immunoassays, which was estimated \$1.5 Bn in 2015, and protein-based assays have the largest market share 68.8%.^[179] Rapid market growth can be attributed to increasing rate of cardiovascular diseases, rising incidence of cancer, increasing geriatric population, the emergence of personalized medicine, and the need for companion diagnostics to increase safety and efficacy of therapies.

Diagnostics manufacturers are increasingly offering detection technologies with multiplexing capabilities. **Table 1** summarizes the attributes of commercial multiplex assays. The existing market for single-plex assays is mature as these assays are robust, low-cost, and easy to use by laboratory technicians. However, a significant limitation of these assays is that they typically lack the ability to measure more than one target. Another key limitation of these commercial single-plex assays is that the required sample volume becomes high as the number of measurements increases (100 μL per target). However, the samples obtained from human patients are often limited at point-of-care settings, in particular blood samples from infants are scarce. Over the last decade, numerous commercial assays have emerged to resolve workflow and sample volume issues. These commercial assays have multiplexing capabilities that transcend single-plex ELISA and Western blot assays by offering reduction in sample processing steps and time, and lower sample volumes (25–50 μL) with high automation to decrease the risk of measurement errors. Another key attribute of these commercial multiplexed devices is that they maintain dynamic range linearity 3–5 orders of magnitude whereas ELISA loses linearity at several orders of magnitude.^[197] This capability is critical as the concentration of assays within a panel differ significantly, which necessitates a wide linear range. In general, commercial multiplexed products have two mainstream formats. The first multiplexing format involves the immobilization of sensing agents on solid surface in an array format, where each sensing region is spatially separated. This assay format may include 1–5 capture antibodies in each array distributed throughout a 96-well plate. Commercial products in array format include Proteome Profiler (R&D systems) and Quantibody (RayBiotech). The second typical assays format involves the immobilization of fluorescent probes on microspheres, in which each bead represents an assay. The polystyrene microspheres may contain different types and concentrations of coded fluorescent dyes (red and near infrared), which are used to determine the bound analytes. Although marketing claims promise high theoretical multiplexing capacity (up to 500 analytes), cross-reactivity of detection probes may compromise the multiplexing capacity.^[198]

Table 1. Commercial multiplexed optical detection products.

Device	Company	Multiplexing capacity	Principle of operation	Readout	Ref.
xMAP	Luminex	35 targets	Fluorescent microspheres	Fluorescence/flow cytometry	[180]
Triage	Quidel	11 immunoassays	Lateral-flow assay	Fluorescence	[181]
Lyra	Quidel	3 targets	Real-time PCR	Fluorescence	[182]
GeneXpert	Cepheid	6 analytes	Nucleic acid amplification test	Fluorescence	[183]
Ella	ProteinSimple	4 targets	ELISA sandwich immunoassay	Fluorescence	[184]
Quantibody	RayBiotech	600 targets	ELISA array	Fluorescence	[185]
Bio-Plex	BIO-RAD	2 assays	Fluorescent microspheres	Fluorescence/flow cytometry	[186]
MILLIPIX MAP	Merck Millipore	42 analytes	Fluorescent microspheres	Fluorescence/flow cytometry	[187]
ProcartaPlex	ThermoFisher Scientific	65 analytes	Fluorescent microspheres	Fluorescence/flow cytometry	[188]
AriaMx	Agilent Technologies	4 targets	Real-time PCR	Fluorescence	[189]
Alere q	Abbott	2 targets	Real-time PCR	Fluorescence	[190]
QuantiNova	Qiagen	5 targets	Real-time PCR	Fluorescence	[191]
LightCycler	Roche	5 targets	Real-time PCR	Fluorescence	[192]
FirePlex	Abcam	17 analytes	Immunoassay	Fluorescence/flow cytometry	[193]
16-plex assays	Quansys Biosciences	16 biomarkers	Quantitative ELISA	Chemiluminescence	[194]
Ciraplex	Aushon BioSystems	10 analytes	ELISA	Chemiluminescence	[195]
Proteome Profiler	R&D systems	49 proteins	Antibody array	Chemiluminescence	[196]

One of the successful multiplexed diagnostic companies, Luminex Corporation (Austin, TX), was founded in 1995 and floated to the stock exchange in 2000. Luminex manufacturers multiplexed assays for application in biomedical research, clinical diagnostics, drug discovery, genetic analysis, biothreat identification, and food safety. Their major product lines include xMAP, xTAG, MAGPIX, Luminex 100/200, FLEXMAP 3D, NxTAG, and ARIES. Their xMAP platform allows multiplexing biological assays based on individually functionalized fluorescent microspheres.^[180] Labeled microspheres can be analyzed by laser excitation in a flow cytometry device in a multiplexed manner. Luminex owns 550 issued patents or applications, in which 124 were issued in the United States for its xMAP platform. In 2008, Luminex received FDA 510(k) approval for its xTAG Respiratory Viral Panel that tests for 12 respiratory viruses at clinical settings.^[199,200] Additionally, Luminex obtained a CE mark in the European Union for its xTAG Gastrointestinal Pathogen Panel.^[201] The company has formed over 70 partnerships including ThermoFisher Scientific and Bio-Rad to broaden the applications in their portfolio and generate license revenues.^[202] In 2016, Merck marketed MILLIPIX MAP Equine-specific multiplex assay that measures 27 cytokines and provides diagnostic data about immune response, inflammation, and physiology.^[203] The revenues of Luminex increased from \$238 Mn in 2015 to \$306 Mn in 2017, where their molecular diagnostics portfolio generated 52.9% of the total revenue.^[204] The company reported a gross margin of 64% and an operating margin of 12% in 2018. Luminex is projected to have stable growth in the upcoming decade due to its expanding product portfolio, strong partnerships, and its robust position in the healthcare reimbursement scheme in the United States.

Abbott Laboratories (Lake Bluff, IL), founded in 1888, is a market leader in in vitro diagnostics including immunoassays and blood tests. The company had a robust multiplexed product

line including the electrochemical i-STAT system, which can run up to 13 blood assays within a single cartridge.^[205,206] In 2017, Abbott acquired point-of-care diagnostic device manufacturer Alere for \$5.3 Bn to strengthen its point-of-care diagnostic device portfolio.^[207] For example, Alere q is a multiplex qualitative nucleic acid amplification test that can identify HIV 1 groups M/N and O, and type 2 in blood and plasma samples.^[192] In 2017, Abbott has reported \$7 billion in diagnostics sales, in which \$2.5 billion was in point-of-care testing.

Cepheid (Sunnyvale, CA), founded in 1996, is a manufacturer of molecular diagnostic systems. The company's core multiplexed diagnostic technologies allow rapid and automated testing of genetic diseases with primary applications in healthcare-associated infections, infectious diseases, sexually transmitted diseases, and oncology. As of 2018, Cepheid markets 17 U.S. FDA approved clinical in vitro diagnostic tests in the United States and 23 tests internationally.^[208] Their core platform (GeneXpert) performs automated and multiplexed real-time PCR measurements of up to six biomarkers using fluorescent detection.^[209] Danaher Corporation (Washington, DC) has acquired Cepheid Inc. for \$4 Bn in 2016.^[210] Before its acquisition, Cepheid reported \$470 Mn in revenues in 2014 and \$538 Mn in 2015.^[211] Cepheid has sold over 10 000 GeneXpert systems.^[212] A key success of the company's flagship platform GeneXpert could be attributed to strong collaborations and endorsements by international partners and healthcare systems including World Health Organization (WHO), United States Agency for International Development (USAID), and National Health Service (NHS) in the United Kingdom.^[213]

The successful adoption of commercial multiplexed devices requires robust and low-cost analytical platforms consisting of validated and optimized analyte/target panels. Platforms that offer results from unprocessed human samples to results with

a high degree of automation at low cost are still a roadblock in the widespread use of multiplexed platforms. The ability to run multiplexed assays with low volumes of samples using finger-prick blood samples will be a key milestone in the wide adoption of such multiplexed commercial devices. Furthermore, the robustness of these platforms is critical, particularly in resource-limited settings, where the ambient conditions (e.g., temperature, moisture) significantly vary. Beyond being commercially viable at an affordable price point, these multiplex assays need to be clinically validated. Although numerous target analytes have been identified in the literature for diseases including cancer, the usefulness of a handful of biomarkers has been proven in randomized clinical trials to have significance in the treatment decision-making process. Hence, technical validation of the multiplex assays as well as the establishment of clinical significance should be an integral part of assay development.

7. Conclusion and Discussion

Multiplex optical assays enable point-of-care diagnostics and research at low cost with high parameter measurements within compact forms. Both high-tech industry and academic labs are interested in the development of assays and peripheral devices for higher multiplexing capacity. While academic labs utilize a wide variety of tools from optical, chemical, mechanical, and electrical operation principles, companies mostly leverage relatively straightforward methods with bead assays and protein arrays with fluorescent and chemiluminescent detection modalities. Robustness and unit cost of research grade multiplex devices should be improved to meet the industry standards. Clinicians and medical experts need extensive training to operate multiplex devices, and make predictive models using advanced algorithms and crowd-sourced user networks. Instead of single-plex devices in clinics, multiplex ones should take their place to increase the accuracy of diagnosis. Manufacturing challenges of highly multiplexed assays partially impede the progress in the field deployable devices. Cross-reactivity of analyte detection mechanisms remains one of the key limitations and chemical advances will overcome these challenges in the near future. Despite being in its infancy, multiplex assays will impact early diagnosis of diseases and empowering citizen scientists for on-site research.

Acknowledgements

A.F.C. and A.E.C. contributed equally to this work. A.F.C. holds a Career Award at the Scientific Interface from Burroughs Wellcome Fund. A.E.C. acknowledges Izmir Biomedicine and Genome Center Start-Up Research Grant. A.F.C. and A.E.C. conceived and led the study and wrote the manuscript. S.N.T. contributed to the electrochemical assays. A.K.Y. contributed to the marketing section and edited the manuscript.

Conflict of Interest

The authors declare no conflict of interest.

Keywords

diagnostic devices, digital analysis, mobile health, multiplex devices, optical assays, point-of-care, portable devices

Received: August 16, 2018

Revised: October 10, 2018

Published online: December 4, 2018

- [1] S. R. Steinhubl, E. D. Muse, E. J. Topol, *Sci. Transl. Med.* **2015**, *7*, 283rv3.
- [2] J. S. Gootenberg, O. O. Abudayyeh, M. J. Kellner, J. Joung, J. J. Collins, F. Zhang, *Science* **2018**, *360*, 439.
- [3] Q. Wei, W. Luo, S. Chiang, T. Kappel, C. Mejia, D. Tseng, R. Y. L. Chan, E. Yan, H. Qi, F. Shabbir, H. Ozkan, S. Feng, A. Ozcan, *ACS Nano* **2014**, *8*, 12725.
- [4] W. Gao, S. Emaminejad, H. Y. Y. Nyein, S. Challa, K. Chen, A. Peck, H. M. Fahad, H. Ota, H. Shiraki, D. Kiriya, D.-H. Lien, G. A. Brooks, R. W. Davis, A. Javey, *Nature* **2016**, *529*, 509.
- [5] T. Laksanasopin, T. W. Guo, S. Nayak, A. A. Sridhara, S. Xie, O. O. Olowookere, P. Cadinu, F. Meng, N. H. Chee, J. Kim, C. D. Chin, E. Muniyazesa, P. Mugwaneza, A. J. Rai, V. Mugisha, A. R. Castro, D. Steinmiller, V. Linder, J. E. Justman, S. Nsanjimana, S. K. Sia, *Sci. Transl. Med.* **2015**, *7*, 273re1.
- [6] J. S. Cybulski, J. Clements, M. Prakash, *PLoS One* **2014**, *9*, e98781.
- [7] H. Mukundarajan, F. J. H. Hol, E. A. Castillo, C. Newby, M. Prakash, Using mobile phones as acoustic sensors for high-throughput mosquito surveillance, <https://doi.org/10.7554/eLife.27854>; <https://elifesciences.org/articles/27854> (accessed: July 2018).
- [8] S. H. Yun, S. J. J. Kwok, *Nat. Biomed. Eng.* **2017**, *1*, 0008.
- [9] X. Wang, O. S. Wolfbeis, *Anal. Chem.* **2016**, *88*, 203.
- [10] A. Leung, P. M. Shankar, R. Mutharasan, *Sens. Actuators, B* **2007**, *125*, 688.
- [11] Z. Xiao-hong, L. Lan-hua, X. Wei-qi, S. Bao-dong, S. Jian-wu, H. Miao, S. Han-chang, *Sci. Rep.* **2014**, *4*, 4572.
- [12] R. Xiao, Z. Rong, S. Chen, W. Chen, S. Wang, *RSC Adv.* **2014**, *4*, 36125.
- [13] S.-H. Ohk, A. K. Bhunia, *Food Microbiol.* **2013**, *33*, 166.
- [14] G. A. Posthuma-Trumpie, J. Korf, A. van Amerongen, *Anal. Bioanal. Chem.* **2009**, *393*, 569.
- [15] O. Mudanyali, S. Dimitrov, U. Sikora, S. Padmanabhan, I. Navruz, A. Ozcan, *Lab Chip* **2012**, *12*, 2678.
- [16] Y. Zhao, H. Wang, P. Zhang, C. Sun, X. Wang, X. Wang, R. Yang, C. Wang, L. Zhou, *Sci. Rep.* **2016**, *6*, 21342.
- [17] Z. Lu, D. O'Dell, B. Srinivasan, E. Rey, R. Wang, S. Vemulapati, S. Mehta, D. Erickson, *Proc. Natl. Acad. Sci. USA* **2017**, *114*, 13513.
- [18] D. Kim, Q. Wei, D. H. Kim, D. Tseng, J. Zhang, E. Pan, O. Garner, A. Ozcan, D. Di Carlo, *Anal. Chem.* **2018**, *90*, 690.
- [19] J. E. Kong, Q. Wei, D. Tseng, J. Zhang, E. Pan, M. Lewinski, O. B. Garner, A. Ozcan, D. Di Carlo, *ACS Nano* **2017**, *11*, 2934.
- [20] B. Berg, B. Cortazar, D. Tseng, H. Ozkan, S. Feng, Q. Wei, R. Y.-L. Chan, J. Burbano, Q. Farooqui, M. Lewinski, D. Di Carlo, O. B. Garner, A. Ozcan, *ACS Nano* **2015**, *9*, 7857.
- [21] H. Yan, Y. Zhu, Y. Zhang, L. Wang, J. Chen, Y. Lu, Y. Xu, W. Xing, *Sci. Rep.* **2017**, *7*, 1460.
- [22] J. Y. Park, L. J. Kricka, *Anal. Bioanal. Chem.* **2014**, *406*, 5631.
- [23] J. Yu, L. Ge, J. Huang, S. Wang, S. Ge, *Lab Chip* **2011**, *11*, 1286.
- [24] A. Ozcan, E. McLeod, *Annu. Rev. Biomed. Eng.* **2016**, *18*, 77.
- [25] A. Bhattacharyya, C. M. Klapperich, *Biomed. Microdevices* **2007**, *9*, 245.

- [26] Y. Liu, W. Shen, Q. Li, J. Shu, L. Gao, M. Ma, W. Wang, H. Cui, *Nat. Commun.* **2017**, *8*, 1003.
- [27] A. Roda, E. Michelini, L. Cevenini, D. Calabria, M. M. Calabretta, P. Simoni, *Anal. Chem.* **2014**, *86*, 7299.
- [28] M. Zangheri, L. Cevenini, L. Anfossi, C. Baggiani, P. Simoni, F. Di Nardo, A. Roda, *Biosens. Bioelectron.* **2015**, *64*, 63.
- [29] W. Gao, C. Wang, K. Muzyka, S. A. Kitte, J. Li, W. Zhang, G. Xu, *Anal. Chem.* **2017**, *89*, 6160.
- [30] J. Heber, *Nature* **2009**, *461*, 720.
- [31] L. Martín-Moreno, F. J. García-Vidal, H. J. Lezec, A. Degiron, T. W. Ebbesen, *Phys. Rev. Lett.* **2003**, *90*, 167401.
- [32] J. N. Anker, W. P. Hall, O. Lyandres, N. C. Shah, J. Zhao, R. P. Van Duyne, *Nat. Mater.* **2008**, *7*, 442.
- [33] N. Nath, A. Chilkoti, *Anal. Chem.* **2004**, *76*, 5370.
- [34] J. Homola, *Chem. Rev.* **2008**, *108*, 462.
- [35] D. Zhang, Q. Liu, *Biosens. Bioelectron.* **2016**, *75*, 273.
- [36] Y. Liu, Q. Liu, S. Chen, F. Cheng, H. Wang, W. Peng, *Sci. Rep.* **2015**, *5*, 12864.
- [37] A. A. Yanik, A. E. Cetin, M. Huang, A. Artar, S. H. Mousavi, A. Khanikae, J. H. Connor, G. Shvets, H. Altug, *Proc. Natl. Acad. Sci. USA* **2011**, *108*, 11784.
- [38] F. Hao, Y. Sonnefraud, P. V. Dorpe, S. A. Maier, N. J. Halas, P. Nordlander, *Nano Lett.* **2008**, *8*, 3983.
- [39] T. W. Ebbesen, H. J. Lezec, H. F. Ghaemi, T. Thio, P. A. Wolff, *Nature* **1998**, *391*, 667.
- [40] A. A. Yanik, M. Huang, O. Kamohara, A. Artar, T. W. Geisbert, J. H. Connor, H. Altug, *Nano Lett.* **2010**, *10*, 4962.
- [41] P. Lalanne, J. C. Rodier, J. P. Hugonin, *J. Opt. A: Pure Appl. Opt.* **2005**, *7*, 422.
- [42] T.-Y. Chang, M. Huang, A. A. Yanik, H.-Y. Tsai, P. Shi, S. Aksu, M. F. Yanik, H. Altug, *Lab Chip* **2011**, *11*, 3596.
- [43] A. E. Cetin, A. F. Coskun, B. C. Galarreta, M. Huang, D. Herman, A. Ozcan, H. Altug, *Light: Sci. Appl.* **2014**, *3*, e122.
- [44] A. F. Coskun, A. E. Cetin, B. C. Galarreta, D. A. Alvarez, H. Altug, A. Ozcan, *Sci. Rep.* **2015**, *4*, 6789.
- [45] Z. S. Ballard, D. Shir, A. Bhardwaj, S. Bazargan, S. Sathianathan, A. Ozcan, *ACS Nano* **2017**, *11*, 2266.
- [46] C. Monat, P. Domachuk, B. J. Eggleton, *Nat. Photonics* **2007**, *1*, 106.
- [47] A. Ymeti, J. Greve, P. V. Lambeck, T. Wink, van Hövell, Beumer, R. R. Wijn, R. G. Heideman, V. Subramaniam, J. S. Kanger, *Nano Lett.* **2007**, *7*, 394.
- [48] A. Ymeti, J. S. Kanger, J. Greve, G. A. J. Besselink, P. V. Lambeck, R. Wijn, R. G. Heideman, *Biosens. Bioelectron.* **2005**, *20*, 1417.
- [49] S. Mandal, J. M. Goddard, D. Erickson, *Lab Chip* **2009**, *9*, 2924.
- [50] S. Jahns, M. Bräur, B.-O. Meyer, T. Karrock, S. B. Gutekunst, L. Blohm, C. Selhuber-Unkel, R. Buhmann, Y. Nazirizadeh, M. Gerken, *Biomed. Opt. Express* **2015**, *6*, 3724.
- [51] C.-S. Huang, V. Chaudhery, A. Pokhriyal, S. George, J. Polans, M. Lu, R. Tan, R. C. Zangar, B. T. Cunningham, *Anal. Chem.* **2012**, *84*, 1126.
- [52] M. Li, X. Wu, L. Liu, X. Fan, L. Xu, *Anal. Chem.* **2013**, *85*, 9328.
- [53] C. N. Kotanen, L. Martinez, R. Alvarez, J. W. Simecek, *Sens. Bio-Sens. Res.* **2016**, *8*, 20.
- [54] S. H. Yazdi, I. M. White, *Analyst* **2012**, *138*, 100.
- [55] W. W. Yu, I. M. White, *Anal. Chem.* **2010**, *82*, 9626.
- [56] W. W. Yu, I. M. White, *Analyst* **2013**, *138*, 1020.
- [57] R. Fu, Q. Li, R. Wang, N. Xue, X. Lin, Y. Su, K. Jiang, X. Jin, R. Lin, W. Gan, Y. Lu, G. Huang, *Talanta* **2018**, *181*, 224.
- [58] M. Zhao, X. Wang, G. M. Lawrence, P. Espinoza, D. D. Nolte, *IEEE J. Sel. Top. Quantum Electron.* **2007**, *13*, 1680.
- [59] G. G. Daaboul, P. Gagni, L. Benussi, P. Bettotti, M. Ciani, M. Cretich, D. S. Freedman, R. Ghidoni, A. Y. Ozkumur, C. Piotto, D. Prospero, B. Santini, M. S. Ünlü, M. Chiari, *Sci. Rep.* **2016**, *6*, 37246.
- [60] M. Piliarik, V. Sandoghdar, *Nat. Commun.* **2014**, *5*, 4495.
- [61] D. Gresham, M. J. Dunham, D. Botstein, *Nat. Rev. Genet.* **2008**, *9*, 291.
- [62] J. M. Hall, M. K. Lee, B. Newman, J. E. Morrow, L. A. Anderson, B. Huey, M. C. King, *Science* **1990**, *250*, 1684.
- [63] L. Wu, S. I. Candille, Y. Choi, D. Xie, J. Li-Pook-Tham, H. Tang, M. Snyder, *Nature* **2013**, *499*, 79.
- [64] J. Shendure, G. J. Porreca, N. B. Reppas, X. Lin, J. P. McCutcheon, A. M. Rosenbaum, M. D. Wang, K. Zhang, R. D. Mitra, G. M. Church, *Science* **2005**, *309*, 1728.
- [65] M. Ronaghi, S. Karamohamed, B. Pettersson, M. Uhlén, P. Nyrén, *Anal. Biochem.* **1996**, *242*, 84.
- [66] M. A. Quail, M. Smith, P. Coupland, T. D. Otto, S. R. Harris, T. R. Connor, A. Bertoni, H. P. Swerdlow, Y. Gu, *BMC Genomics* **2012**, *13*, 341.
- [67] K. J. McKernan, H. E. Peckham, G. L. Costa, S. F. McLaughlin, Y. Fu, E. F. Tsung, C. R. Clouser, C. Duncan, J. K. Ichikawa, C. C. Lee, Z. Zhang, S. S. Ranade, E. T. Dimalanta, F. C. Hyland, T. D. Sokolsky, L. Zhang, A. Sheridan, H. Fu, C. L. Hendrickson, B. Li, L. Kotler, J. R. Stuart, J. A. Malek, J. M. Manning, A. A. Antipova, D. S. Perez, M. P. Moore, K. C. Hayashibara, M. R. Lyons, R. E. Beaudoin, B. E. Coleman, M. W. Laptewicz, A. E. Sannicandro, M. D. Rhodes, R. K. Gottimukkala, S. Yang, V. Bafna, A. Bashir, A. MacBride, C. Alkan, J. M. Kidd, E. E. Eichler, M. G. Reese, F. M. D. L. Vega, A. P. Blanchard, *Genome Res.* **2009**, *19*, 1527.
- [68] H. Lu, F. Giordano, Z. Ning, *Genomics, Proteomics Bioinf.* **2016**, *14*, 265.
- [69] M. Kühnemund, Q. Wei, E. Darai, Y. Wang, I. Hernández-Neuta, Z. Yang, D. Tseng, A. Ahlford, L. Mathot, T. Sjöblom, A. Ozcan, M. Nilsson, *Nat. Commun.* **2017**, *8*, 13913.
- [70] A. E. Cetin, P. Iyidogan, Y. Hayashi, M. Wallen, K. Vijayan, E. Tu, M. Nguyen, A. Oliphant, *ACS Sens.* **2018**, *3*, 561.
- [71] T. P. Burg, M. Godin, S. M. Knudsen, W. Shen, G. Carlson, J. S. Foster, K. Babcock, S. R. Manalis, *Nature* **2007**, *446*, 1066.
- [72] D. A. Raorane, M. D. Lim, F. F. Chen, C. S. Craik, A. Majumdar, *Nano Lett.* **2008**, *8*, 2968.
- [73] M. M. Stevens, C. L. Maire, N. Chou, M. A. Murakami, D. S. Knoff, Y. Kikuchi, R. J. Kimmerling, H. Liu, S. Haidar, N. L. Calistri, N. Cermak, S. Olcum, N. A. Cordero, A. Idbaih, P. Y. Wen, D. M. Weinstock, K. L. Ligon, S. R. Manalis, *Nat. Biotechnol.* **2016**, *34*, 1161.
- [74] N. Cermak, S. Olcum, F. F. Delgado, S. C. Wasserman, K. R. Payer, M. A. Murakami, S. M. Knudsen, R. J. Kimmerling, M. M. Stevens, Y. Kikuchi, A. Sandikci, M. Ogawa, V. Agache, F. Baléras, D. M. Weinstock, S. R. Manalis, *Nat. Biotechnol.* **2016**, *34*, 1052.
- [75] A. E. Cetin, M. M. Stevens, N. L. Calistri, M. Fulciniti, S. Olcum, R. J. Kimmerling, N. C. Munshi, S. R. Manalis, *Nat. Commun.* **2017**, *8*, 1613.
- [76] N. Cermak, J. W. Becker, S. M. Knudsen, S. W. Chisholm, S. R. Manalis, M. F. Polz, *ISME J.* **2017**, *11*, 825.
- [77] M. R. Luskin, M. A. Murakami, S. R. Manalis, D. M. Weinstock, *Nat. Rev. Cancer* **2018**, *18*, 255.
- [78] A. K. Bryan, A. Goranov, A. Amon, S. R. Manalis, *Proc. Natl. Acad. Sci. USA* **2010**, *107*, 999.
- [79] K. Park, L. J. Millet, N. Kim, H. Li, X. Jin, G. Popescu, N. R. Aluru, K. J. Hsia, R. Bashir, *Proc. Natl. Acad. Sci. USA* **2010**, *107*, 20691.
- [80] M. Cavey, T. Lecuit, *Cold Spring Harbor Perspect. Biol.* **2009**, *1*, a002998.
- [81] O. Cakmak, E. Ermeck, N. Kilinc, S. Bulut, I. Baris, I. H. Kavakli, G. G. Yaralioglu, H. Urey, *Lab Chip* **2015**, *15*, 113.
- [82] K. Takahashi, H. Oyama, N. Misawa, K. Okumura, M. Ishida, K. Sawada, *Sens. Actuators, B* **2013**, *188*, 393.
- [83] T. Kartanas, V. Ostanin, P. K. Challa, R. Daly, J. Charmet, T. P. J. Knowles, *Anal. Chem.* **2017**, *89*, 11929.

- [84] D. Zhang, Y. Lu, Q. Zhang, L. Liu, S. Li, Y. Yao, J. Jiang, G. L. Liu, Q. Liu, *Sens. Actuators, B* **2016**, 222, 994.
- [85] J. Gao, L. Jeffries, K. E. Mach, D. W. Craft, N. J. Thomas, V. Gau, J. C. Liao, P. K. Wong, *SLAS Technol.* **2017**, 22, 466.
- [86] C. Zhao, M. M. Thuo, X. Liu, *Sci. Technol. Adv. Mater.* **2013**, 14, 5.
- [87] D. Kinnamon, R. Ghanta, K.-C. Lin, S. Muthukumar, S. Prasad, *Sci. Rep.* **2017**, 7, 13312.
- [88] G. Y. Çiftçi, E. Şenkuytu, S. E. İncir, F. Yuksel, Z. Ölçer, T. Yıldırım, A. Kılıç, Y. Uludağ, *Biosens. Bioelectron.* **2016**, 80, 331.
- [89] U. Christians, J. Klepacki, T. Shokati, J. Klawitter, J. Klawitter, *Microchem. J.* **2012**, 105, 32.
- [90] D. T. Snyder, C. J. Pulliam, Z. Ouyang, R. G. Cooks, *Anal. Chem.* **2016**, 88, 2.
- [91] L. Gao, Q. Song, G. E. Patterson, R. G. Cooks, Z. Ouyang, *Anal. Chem.* **2006**, 78, 5994.
- [92] L. Li, T.-C. Chen, Y. Ren, P. I. Hendricks, R. G. Cooks, Z. Ouyang, *Anal. Chem.* **2014**, 86, 2909.
- [93] A. E. Kirby, N. M. Lafrenière, B. Seale, P. I. Hendricks, R. G. Cooks, A. R. Wheeler, *Anal. Chem.* **2014**, 86, 6121.
- [94] Y. Zhai, Y. Feng, Y. Wei, Y. Wang, W. Xu, *Analyst* **2015**, 140, 3406.
- [95] X. Meng, X. Zhang, Y. Zhai, W. Xu, *Instruments* **2018**, 2, 2.
- [96] Y. Zhai, X. Zhang, H. Xu, Y. Zheng, T. Yuan, W. Xu, *Anal. Chem.* **2017**, 89, 4177.
- [97] M. Yang, T.-Y. Kim, H.-C. Hwang, S.-K. Yi, D.-H. Kim, *J. Am. Soc. Mass Spectrom.* **2008**, 19, 1442.
- [98] P. I. Hendricks, J. K. Dalglish, J. T. Shelley, M. A. Kirleis, M. T. McNicholas, L. Li, T.-C. Chen, C.-H. Chen, J. S. Duncan, F. Boudreau, R. J. Noll, J. P. Denton, T. A. Roach, Z. Ouyang, R. G. Cooks, *Anal. Chem.* **2014**, 86, 2900.
- [99] F. Karouia, K. Peyvan, A. Pohorille, *Biotechnol. Adv.* **2017**, 35, 905.
- [100] J. Zhang, J. Rector, J. Q. Lin, J. H. Young, M. Sans, N. Katta, N. Giese, W. Yu, C. Nagi, J. Suliburk, J. Liu, A. Bensussan, R. J. DeHoog, K. Y. Garza, B. Ludolph, A. G. Sorace, A. Syed, A. Zahedivash, T. E. Milner, L. S. Eberlin, *Sci. Transl. Med.* **2017**, 9, eaan3968.
- [101] M. Ismail, M. Baumert, D. Stevenson, J. Watts, R. Webb, C. Costa, F. Robinson, M. Bailey, *Anal. Methods* **2017**, 9, 1839.
- [102] P. Yager, G. J. Domingo, J. Gerdes, *Annu. Rev. Biomed. Eng.* **2008**, 10, 107.
- [103] S. A. Boppert, R. Richards-Kortum, *Sci. Transl. Med.* **2014**, 6, 253rv2.
- [104] H. Zhu, S. O. Isikman, O. Mudanyali, A. Greenbaum, A. Ozcan, *Lab Chip* **2012**, 13, 51.
- [105] C. W. Pirstill, G. L. Coté, *Sci. Rep.* **2015**, 5, 13368.
- [106] I. I. Bogoch, H. C. Koydemir, D. Tseng, R. K. D. Ephraim, E. Duah, J. Tee, J. R. Andrews, A. Ozcan, *Am. J. Trop. Med. Hyg.* **2017**, 96, 1468.
- [107] M. V. D'Ambrosio, M. Bakalar, S. Bennuru, C. Reber, A. Skandarajah, L. Nilsson, N. Switz, J. Kamgno, S. Pion, M. Boussinesq, T. B. Nutman, D. A. Fletcher, *Sci. Transl. Med.* **2015**, 7, 286re4.
- [108] Z. F. Phillips, M. V. D'Ambrosio, L. Tian, J. J. Rulison, H. S. Patel, N. Sadras, A. V. Gande, N. A. Switz, D. A. Fletcher, L. Waller, *PLoS One* **2015**, 10, e0124938.
- [109] A. Ozcan, *Lab Chip* **2014**, 14, 3187.
- [110] M. K. Kanakasabapathy, M. Sadasivam, A. Singh, C. Preston, P. Thirumalaraju, M. Venkataraman, C. L. Bormann, M. S. Draz, J. C. Petrozza, H. Shafee, *Sci. Transl. Med.* **2017**, 9, eaai7863.
- [111] A. F. Coskun, R. Nagi, K. Sadeghi, S. Phillips, A. Ozcan, *Lab Chip* **2013**, 13, 4231.
- [112] S. K. Vashist, E. M. Schneider, J. H. T. Luong, *Diagnostics* **2014**, 4, 104.
- [113] X. Li, J. Dunn, D. Salins, G. Zhou, W. Zhou, S. M. S.-F. Rose, D. Perelman, E. Colbert, R. Runge, S. Rego, R. Sonecha, S. Datta, T. McLaughlin, M. P. Snyder, *PLoS Biol.* **2017**, 15, e2001402.
- [114] N. D. Price, A. T. Magis, J. C. Earls, G. Glusman, R. Levy, C. Lausted, D. T. McDonald, U. Kusebauch, C. L. Moss, Y. Zhou, S. Qin, R. L. Moritz, K. Brogaard, G. S. Omenn, J. C. Lovejoy, L. Hood, *Nat. Biotechnol.* **2017**, 35, 747.
- [115] S. Rebe Raz, H. Liu, W. Norde, M. G. E. G. Bremer, *Anal. Chem.* **2010**, 82, 8485.
- [116] H. Liu, R. Malhotra, M. W. Pecuh, J. F. Rusling, *Anal. Chem.* **2010**, 82, 5865.
- [117] R. E. Poms, E. Anklam, M. Kuhn, *J. AOAC Int.* **2004**, 87, 1391.
- [118] D. Croote, S. R. Quake, *NPJ Syst. Biol. Appl.* **2016**, 2, 16022.
- [119] A. F. Coskun, J. Wong, D. Khodadadi, R. Nagi, A. Tey, A. Ozcan, *Lab Chip* **2013**, 13, 636.
- [120] A. J. Das, A. Wahi, I. Kothari, R. Raskar, *Sci. Rep.* **2016**, 6, 32504.
- [121] B. Srinivasan, D. O'Dell, J. L. Finkelstein, S. Lee, D. Erickson, S. Mehta, *Biosens. Bioelectron.* **2018**, 99, 115.
- [122] S. Lee, B. Srinivasan, S. Vemulapati, S. Mehta, D. Erickson, *Lab Chip* **2016**, 16, 2408.
- [123] S. Lee, D. O'Dell, J. Hohenstein, S. Colt, S. Mehta, D. Erickson, *Sci. Rep.* **2016**, 6, 28237.
- [124] S. A. Sajjadi, G. Zolfaghari, H. Adab, A. Allahabadi, M. Delsouz, *MethodsX* **2017**, 4, 372.
- [125] C. Orr, R. A. Martin, *Rev. Sci. Instrum.* **1958**, 29, 129.
- [126] D. Broßell, S. Tröller, N. Dziurawitz, S. Plitzko, G. Linsel, C. Asbach, N. Azong-Wara, H. Fissan, A. Schmidt-Ott, *J. Aerosol Sci.* **2013**, 63, 75.
- [127] Y.-C. Wu, A. Shiledar, Y.-C. Li, J. Wong, S. Feng, X. Chen, C. Chen, K. Jin, S. Janamian, Z. Yang, Z. S. Ballard, Z. Göröcs, A. Feizi, A. Ozcan, *Light: Sci. Appl.* **2017**, 6, e17046.
- [128] X.-C. Yu, Y. Zhi, S.-J. Tang, B.-B. Li, Q. Gong, C.-W. Qiu, Y.-F. Xiao, *Light: Sci. Appl.* **2018**, 7, 18003.
- [129] J. J. Gooding, *Anal. Chim. Acta* **2006**, 559, 137.
- [130] M. Pohanka, P. Skládal, M. Kroča, *Def. Sci. J.* **2007**, 57, 185.
- [131] M. T. McBride, S. Gammon, M. Pitesky, T. W. O'Brien, T. Smith, J. Aldrich, R. G. Langlois, B. Colston, K. S. Venkateswaran, *Anal. Chem.* **2003**, 75, 1924.
- [132] J. Kirsch, C. Siltanen, Q. Zhou, A. Revzin, A. Simonian, *Chem. Soc. Rev.* **2013**, 42, 8733.
- [133] A. E. Nicogossian, D. F. Pober, S. A. Roy, *Telemed. J. e-Health* **2001**, 7, 1.
- [134] M. F. Toy, S. Richard, J. Kühn, A. Franco-Obregón, M. Egli, C. Depeursinge, *Biomed. Opt. Express* **2012**, 3, 313.
- [135] J. L. Nadeau, M. Bedrossian, C. A. Lindensmith, *Adv. Phys. X* **2018**, 3, 1424032.
- [136] J. A. DuBois, *Point Care* **2010**, 9, 196.
- [137] R. S. H. Istepanian, E. Jovanov, Y. T. Zhang, *IEEE Trans. Inf. Technol. Biomed.* **2004**, 8, 405.
- [138] L. Salka, F. L. Kiechle, *Point Care* **2003**, 2, 114.
- [139] E. Ghafar-Zadeh, *Sensors* **2015**, 15, 3236.
- [140] K. Ming, J. Kim, M. J. Biondi, A. Syed, K. Chen, A. Lam, M. Ostrowski, A. Rebbapragada, J. J. Feld, W. C. W. Chan, *ACS Nano* **2015**, 9, 3060.
- [141] J. Yao, R. Schmitz, S. Warren, *IEEE Trans. Inf. Technol. Biomed.* **2005**, 9, 363.
- [142] A. W. Martinez, S. T. Phillips, E. Carrilho, S. W. Thomas, H. Sindi, G. M. Whitesides, *Anal. Chem.* **2008**, 80, 3699.
- [143] A. J. Sohn, J. M. Hickner, F. Alem, *J. Am. Board Family Med.* **2016**, 29, 371.
- [144] T. P. Mashamba-Thompson, B. Sartorius, P. K. Drain, *BMC Health Serv. Res.* **2018**, 18, 380.
- [145] J. Song, V. Pandian, M. G. Mauk, H. H. Bau, S. Cherry, L. C. Tisi, C. Liu, *Anal. Chem.* **2018**, 90, 4823.
- [146] A. Ibaida, I. Khalil, *IEEE Trans. Biomed. Eng.* **2013**, 60, 3322.
- [147] K. R. King, L. P. Grazette, D. N. Paltoo, J. T. McDevitt, S. K. Sia, P. M. Barrett, F. S. Apple, P. A. Gurbel, R. Weissleder, H. Leeds,

- E. J. Iturriaga, A. K. Rao, B. Adhikari, P. Desvigne-Nickens, Z. S. Galis, P. Libby, *JACC: Basic Transl. Sci.* **2016**, *1*, 73.
- [148] S. Schumacher, J. Nestler, T. Otto, M. Wegener, E. Ehrentreich-Förster, D. Michel, K. Wunderlich, S. Palzer, K. Sohn, A. Weber, M. Burgard, A. Grzesiak, A. Teichert, A. Brandenburg, B. Koger, J. Albers, E. Nebling, F. F. Bier, *Lab Chip* **2012**, *12*, 464.
- [149] A. K. Ellerbee, S. T. Phillips, A. C. Siegel, K. A. Mirica, A. W. Martinez, P. Striehl, N. Jain, M. Prentiss, G. M. Whitesides, *Anal. Chem.* **2009**, *81*, 8447.
- [150] M. A. Hossain, J. Canning, S. Ast, K. Cook, P. J. Rutledge, A. Jamalipour, *Opt. Lett.* **2015**, *40*, 1737.
- [151] R. D. Stedtfeld, D. M. Tourlousse, G. Seyrig, T. M. Stedtfeld, M. Kronlein, S. Price, F. Ahmad, E. Gulari, J. M. Tiedje, S. A. Hashsham, *Lab Chip* **2012**, *12*, 1454.
- [152] L. Shen, J. A. Hagen, I. Papautsky, *Lab Chip* **2012**, *12*, 4240.
- [153] N. R. Pollock, J. P. Rolland, S. Kumar, P. D. Beattie, S. Jain, F. Noubary, V. L. Wong, R. A. Pohlmann, U. S. Ryan, G. M. Whitesides, *Sci. Transl. Med.* **2012**, *4*, 152ra129.
- [154] L. Ge, J. Yan, X. Song, M. Yan, S. Ge, J. Yu, *Biomaterials* **2012**, *33*, 1024.
- [155] G.-J. Geersing, D. B. Toll, K. J. M. Janssen, R. Oudega, M. J. C. Blikman, R. Wijland, K. M. K. de Vooght, A. W. Hoes, K. G. M. Moons, *Clin. Chem.* **2010**, *56*, 1758.
- [156] C. W. E. Hoedemaekers, J. M. T. K. Gunnewiek, M. A. Prinsen, J. L. Willems, J. G. Van der Hoeven, *Crit. Care Med.* **2008**, *36*, 3062.
- [157] N. Spielmann, J. Mauch, C. Madjdpour, M. Schmutz, M. Weiss, T. Haas, *Int. J. Lab. Hematol.* **2012**, *34*, 86.
- [158] S. D. Blacksell, R. G. Jarman, M. S. Bailey, A. Tanganuchitcharnchai, K. Jenjaroen, R. V. Gibbons, D. H. Paris, R. Premaratna, H. J. de Silva, D. G. Laloo, N. P. J. Day, *Clin. Vaccine Immunol.* **2011**, CVI.05285.
- [159] N. G. Schoepp, T. S. Schlappi, M. S. Curtis, S. S. Butkovich, S. Miller, R. M. Humphries, R. F. Ismagilov, *Sci. Transl. Med.* **2017**, *9*, eaal3693.
- [160] F. Shen, B. Sun, J. E. Kreutz, E. K. Davydova, W. Du, P. L. Reddy, L. J. Joseph, R. F. Ismagilov, *J. Am. Chem. Soc.* **2011**, *133*, 17705.
- [161] F. Shen, W. Du, J. E. Kreutz, A. Fok, R. F. Ismagilov, *Lab Chip* **2010**, *10*, 2666.
- [162] J. H. Chen, S. M. Asch, *N. Engl. J. Med.* **2017**, *376*, 2507.
- [163] C. L. Chen, A. Mahjoubfar, L.-C. Tai, I. K. Blaby, A. Huang, K. R. Niazi, B. Jalali, *Sci. Rep.* **2016**, *6*, 21471.
- [164] Y. Jiang, C. Lei, A. Yasumoto, H. Kobayashi, Y. Aisaka, T. Ito, B. Guo, N. Nitta, N. Kutsuna, Y. Ozeki, A. Nakagawa, Y. Yatomi, K. Goda, *Lab Chip* **2017**, *17*, 2426.
- [165] H. Ceylan Koydemir, Z. Gorocs, D. Tseng, B. Cortazar, S. Feng, R. Y. L. Chan, J. Burbano, E. McLeod, A. Ozcan, *Lab Chip* **2015**, *15*, 1284.
- [166] Y. Rivenson, Z. Göröcs, H. Günaydin, Y. Zhang, H. Wang, A. Ozcan, *Optica* **2017**, *4*, 1437.
- [167] Y. Rivenson, H. C. Koydemir, H. Wang, Z. Wei, Z. Ren, H. Günaydin, Y. Zhang, Z. Göröcs, K. Liang, D. Tseng, A. Ozcan, *ACS Photonics* **2018**, *5*, 2354.
- [168] R. Chunara, M. S. Smolinski, J. S. Brownstein, *Curr. Infect. Dis. Rep.* **2013**, *15*, 316.
- [169] J. Ginsberg, M. H. Mohebbi, R. S. Patel, L. Brammer, M. S. Smolinski, L. Brilliant, *Nature* **2009**, *457*, 1012.
- [170] A. F. Dugas, Y.-H. Hsieh, S. R. Levin, J. M. Pines, D. P. Mareiniss, A. Mohareb, C. A. Gaydos, T. M. Perl, R. E. Rothman, *Clin. Infect. Dis.* **2012**, *54*, 463.
- [171] S. Mavandadi, S. Dimitrov, S. Feng, F. Yu, R. Yu, U. Sikora, A. Ozcan, *Lab Chip* **2012**, *12*, 4102.
- [172] S. Mavandadi, S. Feng, F. Yu, S. Dimitrov, R. Yu, A. Ozcan, *Games Health J.* **2012**, *1*, 373.
- [173] V. Curtis, *Appl. Transl. Genomics* **2014**, *3*, 90.
- [174] Multiplexed Diagnostics Market By Product (Reagents & Consumables, Analyzers), By Application (Disease Diagnostics, Molecular Diagnostics, Drug Development), By Technology (Very High Density Multiplexed Assays, High Density Multiplexed Assays, Medium Density Multiplexed Assays, Low Density Multiplexed Assays, Next Generation Sequencing Assays) – Growth, Future Prospects And Competitive Analysis, 2017–2025, Report Code: 58930-01-18, Credence Research, **2018**.
- [175] Multiplex Assays Market by Product (Consumables, Instruments), Type (Nucleic Acid, Protein, Cell), Technology (Flow Cytometry, Luminescence), Application (R&D, Diagnosis), End User (Pharma & Biotech, Reference Laboratory, Hospital) – Global Forecast to 2023, BT 4473, Markets and Markets (accessed: August 2018).
- [176] R. and M. Ltd., Multiplexed Diagnostics Market: Global Industry Analysis, Trends, Market Size and Forecasts up to 2024, ID: 4590657, Research and Markets, **2018**.
- [177] Multiplex Biomarker Imaging Market: North America Expected to be the Most Attractive Regional Market during the Forecast Period: Global Industry Analysis 2012–2016 and Opportunity Assessment 2017–2027, REP-GB-3526, Future Market Insights, 2017 (accessed: August 2018).
- [178] Multiplexed Diagnostics Market (Technologies – Very High Density, High Density, Medium Density, Low Density, and Next Generation Sequencing Assays; Applications – Infectious Disease Diagnostics, Oncology, Autoimmune Diseases, Cardiac Diseases, and Allergies; End Users – Academic Research Institutes, Hospitals, Pharmaceuticals Companies, Clinical Research Organizations, and Diagnostic Laboratories) – Global Industry Analysis, Size, Share, Growth, Trends, and Forecast 2016–2024, Rep ID: TMRGL1719, Transparency Research, **2017**.
- [179] Global Market Study on Multiplex Detection Immunoassay: North America to Dominate the Global Market through 2024, Report code: PMRREP11542, Persistence Market Research, **2016**.
- [180] S. A. Dunbar, *Clin. Chim. Acta* **2006**, *363*, 71.
- [181] H. I. Bang, M.-A. Jang, Y.-W. Lee, *Ann. Lab. Med.* **2017**, *37*, 522.
- [182] P. R. Heaton, M. J. Espy, M. J. Binnicker, *Diagn. Microbiol. Infect. Dis.* **2015**, *81*, 169.
- [183] D. Li, K. Wilkins, A. M. McCollum, L. Osadebe, J. Kabamba, B. Nguete, T. Likafi, M. P. Balilo, R. S. Lushima, J. Malekani, I. K. Damon, M. C. L. Vickery, E. Pukuta, F. Nkawa, S. Karhemere, J.-J. M. Tamfum, E. W. Okitolonda, Y. Li, M. G. Reynolds, *Am. J. Trop. Med. Hyg.* **2017**, *96*, 405.
- [184] M. Dysinger, G. Marusov, S. Fraser, *J. Immunol. Methods* **2017**, *451*, 1.
- [185] H. C. Toh, W.-W. Wang, W. K. Chia, P. Kvistborg, L. Sun, K. Teo, Y. P. Phoon, Y. Soe, S. H. Tan, S. W. Hee, K. F. Foo, S. Ong, W. H. Koo, M.-B. Zocca, M. H. Claesson, *Clin. Cancer Res.* **2009**, *15*, 7726.
- [186] B. Houser, *Arch. Physiol. Biochem.* **2012**, *118*, 192.
- [187] G. V. Denis, P. Sebastiani, K. A. Bertrand, K. J. Strissel, A. H. Tran, J. Slama, N. D. Medina, G. Andrieu, J. R. Palmer, *PLoS One* **2018**, *13*, e0196755.
- [188] M. P. Rodero, A. Tesser, E. Bartok, G. I. Rice, E. D. Mina, M. Depp, B. Beitz, V. Bondet, N. Cagnard, D. Duffy, M. Dussiot, M.-L. Frémond, M. Gattorno, F. Guillem, N. Kitabayashi, F. Porcheray, F. Rieux-Laucat, L. Seabra, C. Ugenti, S. Volpi, L. A. H. Zeef, M.-A. Alyanakian, J. Beltrand, A. M. Bianco, N. Boddaert, C. Brouzes, S. Candon, R. Caorsi, M. Charbit, M. Fabre, F. Faletra, M. Girard, A. Harroche, E. Hartmann, D. Lasne, A. Marcuzzi, B. Neven, P. Nitschke, T. Pascreau, S. Pastore, C. Picard, P. Picco, E. Piscianz, M. Polak, P. Quartier, M. Rabant, G. Stocco, A. Taddio, F. Uetwiller, E. Valencic, D. Voizzi, G. Hartmann, W. Barchet, O. Hermine, B. Bader-Meunier, A. Tommasini, Y. J. Crow, *Nat. Commun.* **2017**, *8*, 2176.

- [189] G. Yang, J. Jones, Y. Jang, C. T. Davis, *Appl. Microbiol. Biotechnol.* **2016**, *100*, 8809.
- [190] I. V. Jani, B. Meggi, N. Mabunda, A. Vubil, N. E. Siteo, O. Tobaiwa, J. I. Quevedo, J. D. Lehe, O. Loquiha, L. Vojnov, T. F. Peter, *JAIDS, J. Acquired Immune Defic. Syndr.* **2014**, *67*, e1.
- [191] Y. Wang, J. Y. S. Tsang, Y. Cui, J. Cui, Y. Lin, S. Zhao, P. T. W. Law, S. Y. Cheung, E. K. O. Ng, G. M. K. Tse, Z. Ke, *Sci. Rep.* **2017**, *7*, 6752.
- [192] M. D. Boer, O. W. Akkerman, M. Vermeer, D. L. J. Hess, H. A. M. Kerstjens, R. M. Anthony, T. S. van der Werf, D. van Soelingen, A. G. M. van der Zanden, *PLoS One* **2018**, *13*, e0190847.
- [193] M. R. Tackett, I. Diwan, *Methods Mol. Biol.* **2017**, *1654*, 209.
- [194] A. Ricciardi, K. Visitsunthorn, J. P. Dalton, M. Ndao, *BMC Infect. Dis.* **2016**, *16*, 112.
- [195] L. A. Krueger, D. C. Beitz, S. B. Humphrey, J. R. Stabel, *J. Dairy Sci.* **2016**, *99*, 9040.
- [196] J.-C. Simard, A. Cesaro, J. Chapeton-Montes, M. Tardif, F. Antoine, D. Girard, P. A. Tessier, *PLoS One* **2013**, *8*, e72138.
- [197] P. J. Tighe, R. R. Ryder, I. Todd, L. C. Fairclough, *Proteomics: Clin. Appl.* **2015**, *9*, 406.
- [198] M. Pla-Roca, R. F. Leulmi, S. Tourekhanova, S. Bergeron, V. Laforte, E. Moreau, S. J. C. Gosline, N. Bertos, M. Hallett, M. Park, D. Juncker, *Mol. Cell. Proteomics* **2012**, *11*, M111.011460.
- [199] C. K. Lee, H. K. Lee, C. W. S. Ng, L. Chiu, J. W. T. Tang, T. P. Loh, E. S. C. Koay, *Ann. Lab. Med.* **2017**, *37*, 267.
- [200] K. Pabbaraju, K. L. Tokaryk, S. Wong, J. D. Fox, *J. Clin. Microbiol.* **2008**, *46*, 3056.
- [201] Luminex's xTAG Gastrointestinal Pathogen Panel Gains CE Mark, Genetic Engineering and Biotechnology News (accessed: August 2018).
- [202] N. H. Shamir, presented at *Cantor Fitzgerald Global Healthcare Conf.*, New York, NY, USA, September **2017**.
- [203] E. M. Martin, K. M. Messenger, M. K. Sheats, S. L. Jones, *Front. Vet. Sci.* **2017**, *4*, <https://doi.org/10.3389/fvets.2017.00160>.
- [204] N. H. Shamir, presented at *36th Annual J. P. Morgan Healthcare Conf., Investor Presentation*, San Francisco, CA, USA, January **2018**.
- [205] B. I. Bodai, M. D. Grandon, S. J. Gilbert, D. J. Littlejohn, K. E. Lemons, R. L. Fellows, M. R. Barry, M. D. Delapp, US4929426A, **1990**.
- [206] K. A. Erickson, P. Wilding, *Clin. Chem.* **1993**, *39*, 283.
- [207] Abbott acquisition of alere set to close on tuesday, October 3, 2017, Press Release, Abbott Laboratories (September 29, 2017).
- [208] Corporate Overview, Press Release, Cepheid, **2018**.
- [209] D. Hillemann, S. Rüscher-Gerdes, C. Boehme, E. Richter, *J. Clin. Microbiol.* **2011**, *49*, 1202.
- [210] Danaher Completes Acquisition of Cepheid, Press Release, Danaher.
- [211] Cepheid | Cepheid Reports Fourth Quarter and Full Year 2015 Results.
- [212] Cepheid | Cepheid Delivers Milestone 10,000th GeneXpert System.
- [213] Cepheid | 2017 launch of new TB test Ultra backed by WHO recommendation.